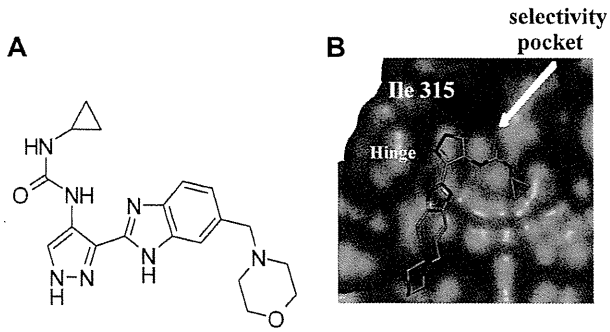

Figure 1. Chemical structure of AT9283 and model of AT9283 bound with ABL. (A) Chemical structure of AT9283. (B) AT9283 does not make a hydrogen bond interaction with T315 in the same way other kinase inhibitors in the class do. The pocket behind the T315 gatekeeper is not occupied by AT9283. Its potency for ABL kinase is not abrogated by mutation of this residue to the bulkier isoleucine (T315I).

with similar potency in the range of 10 to 21nM. The IC_{50} of AT9283 for the BCR-ABL$^-$ parental BaF3 was 103nM, around 5 times higher than that for BaF3 cells harboring wt or mutated BCR-ABL. In addition, we observed that, although multinucleated cells, the hallmark of Aurora B inhibition, were visible microscopically (data not shown), this phenotype did not dominate, and we were able to generate cytotoxic IC_{50} values in the absence of intervention of the polyploid phenotype that maintains cells in a viable state for a longer period of time. These data suggest that additional activities of AT9283, which most likely include BCR-ABL inhibition, are responsible for some of the activity of the compound in vitro.

Similar observations were made in human imatinib-sensitive CML cell lines. These observations are again consistent with the BCR-ABL inhibitory activity of AT9283 contributing to the activity of the compound in CML cell lines harboring the translocation. We observed the dominant Aurora B phenotype of polyploidy in the K562 CML cell line and BCR-ABL$^-$ cell lines such as HL-60, Jurkat, Nalm6, and KG1a. In these cell lines, the dominant phenotype of Aurora B inhibition (polyploidy) was observed in contrast to other CML lines tested. AT9283 was active not only in BaF3/T315I, which was artificially generated, but also in the human CML subclone, KBM-5/STIR, which harbored the T315I mutation (Table 2).

Table 1. Antiproliferative activity of AT9283 in a panel of BaF3 BCR-ABL cell lines

BaF3	AT9283 IC_{50}, nM
Parental (BCR-ABL$^-$)	103
wt p190	16
wt p210	13
Y253F	16
T315I	11
T315A	10
Q252H	21
M351T	18
M294V	18
H396P	21
G250E	12
F317V	14
F317L	15
E255K	13

Y253F indicates tyrosine 253 to phenylalanine; T315A, threonine 315 to alanine; Q252H, glutamine 252 to histidine; M351T, methionine 351 to threonine; M294V, methionine 294 to valine; H396P, histidine 396 to proline; G250E, glycine 250 to glutamic acid; F317V, phenylalanine 317 to valine; and F317L, phenylalanine 317 to leucine.

Table 2. Antiproliferative activity of AT9283 in a panel of human CML cell lines

Cell line	BCR-ABL status	Additional characteristics	IC_{50}, nM
Imatinib sensitive			
BV173	+		55
KU812	+		26
MYL	+		21
KT-1	+		81
KBM-5	+		84
MEG-01	+		31
K562	+		Polyploidy at 100
Imatinib resistant			
KBM-5/STIR	+	T315I mutation	16
BV173/shBim	+	Bim knockdown	12
HL60	–		Polyploidy at 30
Jurkat	–		Polyploidy at 500
Nalm6	–		Polyploidy at 140
KG1a	–		Polyploidy at 55

Induction of apoptosis and alteration of cell cycle by AT9283

Apoptosis was dose-dependently induced in all cell lines tested, including BaF3/wt-BCR-ABL^{p210}, BaF3/T315I, BaF3/E255K, K562, and BV173. AT9283 induced fewer apoptotic cells in K562 than the other 4 CML cell lines (supplemental Figure 2). Exposure of K562 cells to cytotoxic IC_{50} concentrations (100nM) of AT9283 resulted in the appearance of a large multinucleated cell population. Interestingly, exposure of the other 4 cell lines tested to their respective cytotoxic IC_{50} concentrations of AT9283 did not result in the appearance of polyploid cells. The dominant effect in 7 BCR-ABL$^+$ cell lines except K562 was the induction of apoptosis as indicated by a significantly larger increase in subG$_1$ DNA compared with 3 BCR-ABL$^-$ cell lines at 24 hours and 48 hours (supplemental Figures 3-4). If the concentration of AT9283 was increased to 3 times their respective IC_{50} concentrations, a small polyploid population could be observed in the BaF3 and BV173 cells, but the dominant phenotype remained an increase in the apoptotic population. These observations are consistent with the Aurora inhibitory activity of the compound dominating in BCR-ABL lines and K562 cells, resulting in apoptosis only after an increased exposure time and several rounds of endo-reduplication. In the BaF3/BCR-ABL and in other human CML cell lines, AT9283 results in an early apoptotic response in the absence of the classical Aurora inhibitory phenotype. This response is most likely due to the contribution of ABL inhibition in these cells (supplemental Figures 3-4).

Mechanism of action of AT9283 in BCR-ABL$^+$ cell lines

After 24 hours of incubation of BaF3/BCR-ABL wt or T315I cells with AT9283, inhibition of the signaling pathway downstream of Aurora B and BCR-ABL were examined. Phosphorylation of the Aurora B substrate, pHH3 was inhibited by AT9283 at concentrations greater than 30nM in all cell lines examined (Figure 2). Activity of the BCR-ABL fusion was determined by phosphorylation of the substrate STAT5. AT9283 inhibited phosphorylation of STAT5 at concentrations above 300nM in both BaF3/wt-BCR-ABL^{p210} and BaF3/T315I (Figure 2). Similar data were obtained in the human CML cell lines BV173 and K562 above 300nM and 1000nM, respectively. AT9283 inhibited phosphorylation of the BCR-ABL substrate CrkL only in BV173 at concentrations consistent with inhibition of pSTAT5. Incomplete inhibition of phosphorylation of AKT was observed in all cell lines with the most striking

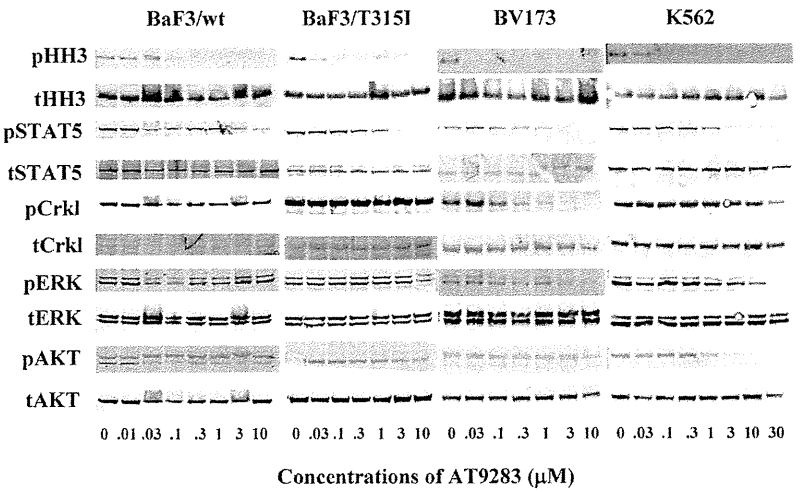

Figure 2. Mechanism of action of AT9283 in BaF3 BCR-ABL cells and human CML cell lines. BaF3/wt-BCR-ABL, BaF3/T315I, BV173, and K562 were incubated with the indicated concentration of AT9283, or vehicle control, for 24 hours before preparation for immunoblotting with the indicated antibodies. The blots shown are representative of at least 2 independent experiments in each cell line.

effects observed in BV173 cells and K562 cells above 100nM. Phospho-ERK inhibition was observed in BV173 and K562 cells but only at concentrations above 3000nM (Figure 2). In addition to the analysis of downstream signaling of AT9283 kinase targets, we also examined the effects of AT9283 on the phosphorylation status of BCR-ABL, Aurora A, and Aurora B themselves. AT9283 inhibited phosphorylation of BCR-ABL, Aurora A, and Aurora B in BV173, BCR-ABL$^+$ cells, at 1.0, 0.1, and 0.03μM, respectively (supplemental Figure 5). In Jurkat, BCR-ABL$^-$ cells, AT9283 also inhibited phosphorylation of Aurora A and Aurora B at 0.3 and 0.3μM, respectively (data not shown). AT9283 inhibited the phosphorylation of HH3 and ERK but AKT in 3 BCR-ABL$^-$ cell lines (supplemental Figure 6). These data suggest that of the signaling pathways studied AT9283 inhibits both the Aurora kinases and BCR-ABL/STAT5 signaling pathways. Inhibition of pCrkL was also observed in the human CML cell line BV173. In other cell lines tested this was less clear and probably reflects the fact that CrkL signaling is regulated by different or additional kinases in BaF3/BCR-ABL lines and in the CML line K562. The latter responds to AT9283 in a manner atypical with respect to the other human CML lines tested, perhaps indicating that it harbors additional mutations or signaling aberrations that impinge on its survival and overall response to AT9283.

Effects of AT9283 in normal hematopoietic progenitors and primary CML cells

The number of colony forming units (CFUs) observed after AT9283 treatment of cells derived from 3 healthy individual donors and 3 patients with CML were examined by colony assay at day 14 to day 16. When normal progenitors were treated with 10, 30, 50, 70, and 100nM AT9283, the CFUs were 0.98% (± 0.06%), 0.62% (± 0.01%), 0.35% (± 0.01%), 0.18% (± 0.01%), 0.11% (± 0.1%), and 0% (± 0%) of the control, respectively. Although when primary CML cells were treated with 10, 30, 50, 70, and 100nM AT9283, the CFUs were 0.45% (± 0.1%), 0.23% (± 0.02%), 0.06% (± 0.02%), 0% (± 0%), 0% (± 0%), and 0% (± 0%) of the control, respectively (supplemental Figure 7). These percentages are the mean plus or minus SE between the 3 persons. These findings indicate that AT9283 was approximately 5 times more effective at inhibiting colony formation with cells derived from patients with CML than from healthy volunteers.

In vivo efficacy of AT9283 in subcutaneous BaF3 BCR-ABL xenograft models

Two cycles of 12.5 mg/kg AT9283 daily for 5 days followed by a 2-day break inhibited tumor growth in subcutaneous xenograft models with BaF3 cells transfected with either BCR-ABL wt (Figure 3A) or T315I (Figure 3B) without obvious adverse effects. Moreover, AT9283 inhibited the growth of human CML cell line K562 xenografts in a dose-dependent fashion after twice daily dosing for 5 days in a 7-day period. Tumor regressions were observed at 12.5 mg/kg, the highest dose, with 4 of 8 mice remaining tumor free at 90 days after initiation of treatment (Figure 3C). This dose schedule was optimized in solid tumor xenograft models.[19]

The activity of AT9283 was investigated in intravenously transplanted models with the use of primary BCR-ABL$^+$ blasts isolated from patients with Ph$^+$ ALL who showed imatinib acquired resistance by harboring 2 of the mutations most resistant to common kinase inhibitor therapies, E255K and T315I. Blasts isolated from patients were injected into the tail vein of NOD/SCID mice and allowed to engraft for a period of 7 days. In the case of the BCR-ABL/E255K model animals were dosed with either vehicle or 6.25 mg/kg AT9283 twice daily for 5 days followed by a 2-day break. This schedule was repeated for 4 cycles and resulted in a significant survival advantage of 17 days over control (Figure 4A). Initially a twice daily schedule was used on the basis of past experience with AT9283 and the optimum schedule in nude mice bearing human tumor xenografts derived from solid tumors. In the course of the studies, we determined that a once daily schedule at the indicated doses allowed indefinite continuous dosing with an improved tolerability profile in NOD/SCID mice and at least as good if not better efficacy in the models described. Thus, for the T315I model, animals were dosed once per day at either 10 or 15 mg/kg. In this case animals continued dosing through to the end of the experiment. In this model a significant survival advantage ($P < .01$) of 17 and 23 days for the 10- and 15-mg/kg groups, respectively, was obtained (Figure 4B). Fluorescence-activated cell sorting analysis, performed on the peripheral blood of mice inoculated with leukemic cells, showed that a number of these cells remained even after dosing with AT9283 (data not shown). The numbers of leukemic cells observed was fewer than that in vehicle-treated mice, consistent with the slower progression of the disease in these animals. In addition, we confirmed the existence of

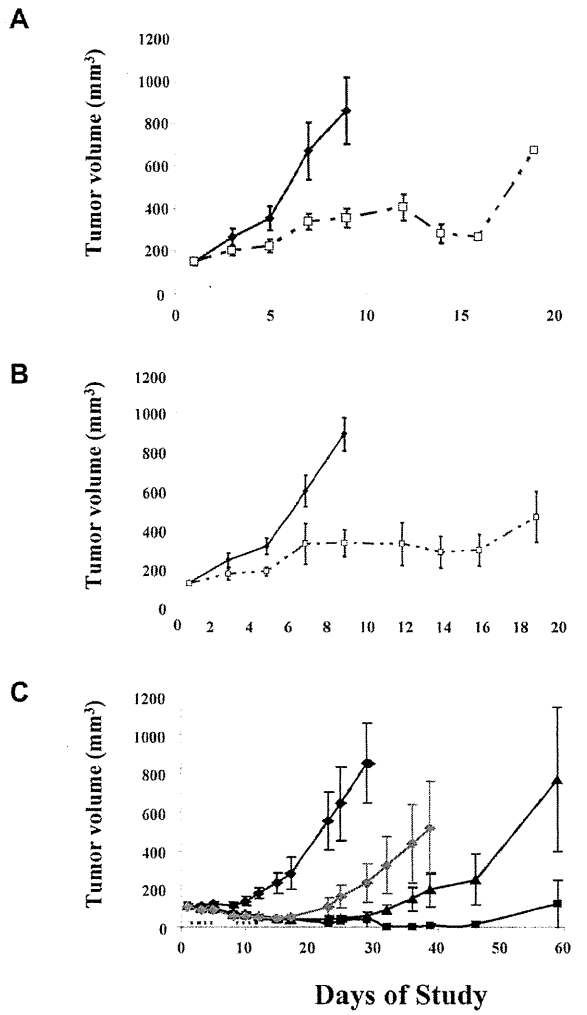

Figure 3. In vivo efficacy of AT9283 in BCR-ABL⁺ cell line xenograft. Nude mice bearing either BaF3/wt-BCR-ABL^{p210} (A) or BaF3/T315I (B) xenografts were administered the indicated doses of AT9283 by the intraperitoneal route. Vehicle (♦) and 12.5 mg/kg AT9283 (□) was dosed twice daily for 5 days followed by a 2-day break. The dose cycle was repeated twice in each case. Nude mice bearing human CML cells, K562 (C) xenografts were also administered the indicated doses of AT9283 by the intraperitoneal route. Vehicle (♦), 12.5 mg/kg (■), 10 mg/kg (□), and 7.5 mg/kg (♦) AT9283 was dosed twice daily for 5 days followed by a 2-day break. The dose cycle was repeated twice in each case. Mean growth curves ± SEs are shown for groups of 8 mice in each instance.

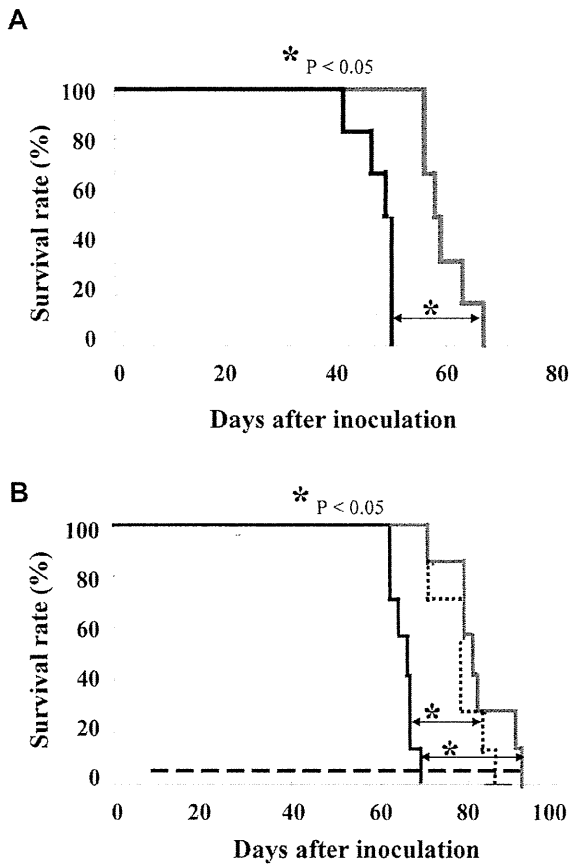

Figure 4. In vivo efficacy of AT9283 in primary samples. Nonlethally irradiated NOD/SCID mice were intravenously inoculated with cells taken from patients with CML harboring BCR-ABL E255K (A) or BCR-ABL T315I (B). Either 6.25 mg/kg AT9283 (gray) or vehicle (black) controlled was administered twice daily (A) on the indicated schedules (- - -). We administered 15 mg/kg AT9283 (gray), 10 mg/kg At9283 (black dot), or vehicle (black) controlled once daily (B) on the indicated schedules (- - -). Kaplan-Meier survival curves show that treatment with 6.25 mg/kg AT9283 twice daily resulted in a significant survival advantage ($P = .008$) over vehicle-treated animals of 17 days in the E255K model. Similarly, in the T315I model 10 mg/kg per day or 15 mg/kg per day AT9283 resulted in a marked survival advantage ($P = .002$).

T315I clones both in peripheral blood of AT9283-treated and vehicle-dosed mice by the modified guanine quenching probe method (supplemental Figure 8). In several mice we performed postmortem examinations for the presence of leukemic cells in liver and spleen with the use of the same method (data not shown). Tissue samples from both vehicle- and AT9283-treated mice were shown to be positive for the T315I clone, showing that, although AT9283 significantly slowed the proliferation of leukemic cells and prolonged the survival of the mice, it could not completely suppress the growth of leukemic cells in this model.

Discussion

To date, at least 90 different point mutations in the BCR-ABL kinase domain have been isolated from patients with BCR-ABL⁺ leukemia who are resistant to imatinib.[25,26] In addition to imatinib, other novel ABL TKIs are ineffective against the T315I mutant clone. This suggests that more patients with the T315I clone will emerge now that treatment with TKIs has become the standard of care in CML. The observation that T315I mutations were most frequently observed in dasatinib-resistant patients appears to support this observation.[27] Some studies have suggested that patients with T315I have a poor prognosis, with a median survival of 12.6 months from the start of imatinib therapy.[28,29] Therefore, there is much interest in developing novel agents effective against BCR-ABL/T315I clone.

To understand the activity of AT9283 versus BCR-ABL/T315I, we must first understand the mechanisms of resistance to existing agents in the adenosine triphosphate–binding pocket of BCR-ABL/T315I (Figure 1; supplemental Figure 1). As the explanations of resistance of ABL/T315I to imatinib, there are 3 hypotheses such as alteration of the 3-dimensional structure of the adenosine triphosphate pocket,[30,31] the consequence of a conformational readjustment necessary to accommodate the mutant residue,[32] and the breakdown of interactions between imatinib and both E286 and

M290.[33] In the case of AT9283, the simplest explanation for the tolerance of the T315I is 2-fold: the lack of any hydrogen bond formed by this compound with the side-chain of T315, and the compound's avoidance of the selectivity pocket behind the gatekeeper residue. Put simply, the binding mode and key interactions formed by AT9283 are probably largely independent of the nature of the residue at position 315 (Figure 1B; supplemental Figure 1).

Note that the structure of the kinase domain of c-ABL in complex with a T315I-sensitive Aurora kinase inhibitor, MK-0457 (formerly VX-680), has already been reported.[34] The inhibition by both MK-0457 and PHA-739358 of the T315I mutant also arises because of their particular binding modes, which also avoid the gatekeeper region.[35] MK-0457 was found to be active against BCR-ABL/T315I,[34] and a phase 2 trial on MK-0457 for patients with CML with T315I showed some efficacy.[36] Unfortunately, the development of MK-0457 was halted for commercial reasons. QTc prolongation[37] or any adverse events was not involved in the closing of the phase 2 study, which confirmed significant activity in patients with T315I. PHA-739358 also has been reported to have strong antiproliferative and proapoptotic activity against BCR-ABL including T315I.[38] A phase 2 trial of PHA-739358 in patients with CML who have relapsed after BCR-ABL therapy is ongoing.

Because AT9283 is a multitargeted inhibitor with activities that include ABL and the Aurora kinases, it is important to understand which activities are key in driving the effects in CML cells. AT9283 inhibited both BCR-ABL and Aurora signaling (Figure 2; supplemental Figures 5-6). In addition, cell death observed in BCR-ABL$^+$ cell lines, treated with AT9283, is consistent with inhibition of BCR-ABL activity and is observed in the absence of the accumulation of large numbers of polyploid cells normally associated with Aurora inhibition in other cell lines. However, we do observe small numbers of multinucleated cells, suggesting that the Aurora activity of AT9283 is manifest in the background (Table 2; supplemental Figures 3-4). AT9283 is multitargeted in nature, and no single activity is the sole driver of its effect. We show potent inhibition of Aurora A and B; however, the BCR-ABL$^+$ cell lines do exhibit a different phenotype to the classic Aurora phenotype described in our previous study.[14] It is this combinatorial nature of the effect that suggests we may have a beneficial effect in the patient population with T315I for which there is at present no effective treatment.

In vivo models of CML have shown activity of AT9283 in a cell line grown as a subcutaneous xenograft (K562; Figure 3) and in models in which leukemic cells harboring E255K or T315I from patients were intravenously inoculated into NOD/SCID mice (Figure 4). In these models, 2 dosing regimens, twice daily and once daily, were used. In the nude mouse, there was no significant difference between twice daily and once daily dosing on tumor growth inhibition or tolerability (data not shown). In primary BCR-ABL$^+$ tumor models a larger AT9283 dose administered once daily was tolerated better than a lower dose administered twice daily with no loss of efficacy. This could relate to the mechanism of action of AT9283 in these CML cells, perhaps indicating that transient, yet complete, inhibition of BCR-ABL signaling is sufficient to drive efficacy. Similar observations have been made for dasatinib.[39,40]

Because of the aggressive nature of the cell growth in these animal models, it is usually not possible for any ABL TKI to suppress completely the growth of leukemic cells engrafted in this manner. However, the survival advantage shown here, although small, is significant and offers hope for AT9283 and its therapeutic potential. For example, an ABL/LYN inhibitor INNO-406 (NS-187) prolonged the survival of mice engrafted with BCR-ABL$^+$ cells in almost the same setting to a similar small yet significant extent showed responses in several imatinib-resistant patients in clinical trials.[41,42] Thus, it is our opinion that the presented survival difference, afterAT9283 treatment in these models, has the potential to reflect clinical benefit.

We show that the colony formation capacity of primary CML cells was inhibited by AT9283 at IC_{50} concentrations that were approximately 5-fold lower than those required to produce the same effect in progenitors from healthy volunteers. In addition, IC_{50} value of AT9283 for parental BaF3 cells was much higher than BCR-ABL$^+$ BaF3 cells, and IC_{50} values of AT9283 for most human CML cell lines, including imatinib-resistant cell lines. In clinical studies we have defined maximum-tolerated doses in patients with refractory solid tumor and patients with leukemia. Pharmacokinetic studies have shown that concentrations of AT9283 achieved in the plasma are consistent with the concentrations required to inhibit BCR-ABL$^+$ cell growth in the studies presented here.[43] In addition, biomarker modulations of a number of targets of AT9283 have been shown in samples taken during the course of these studies. These observations suggest that therapeutically relevant concentrations can be achieved at well-tolerated doses.[43]

On the basis of previous preclinical studies,[18,19] we have already treated 2 patients with TKI-refractory CML in accelerated phase as part of a dose-finding study of AT9283. Although the ABL mutational statuses of these patients were unknown, both patients achieved a hematologic response after treatment with AT9283. The present study strongly suggests that AT9283 has the potential to significantly benefit patients with CML or with Ph$^+$ ALL that is resistant to current forms of therapy. Moreover, AT9283 could be useful for patients bearing T315I clones. Therefore, the efficacy and safety of AT9283 for BCR-ABL$^+$ leukemias warrants further investigation in a clinical setting.

Acknowledgments

We thank Darcey Miller, Jayne Curry, and Kirsty Mallet for the provision of supporting data for these studies and Tom Davies and Valerio Berdini for discussion and interpretation of the BCR-ABL T315I modeling data.

This work was partly supported by Grant-in-Aids for Scientific Research and for JSPS fellows, Global COE Program "Center for Frontier Medicine" from the Ministry of Education, Culture, Sports, Science and Technology (MEXT) of Japan, and by Management Expenses Grants from the Government to the National Cancer Center of Japan.

Authorship

Contribution: R.T. performed research and analyzed data; M.S.S., and S.K. designed and performed research, and wrote the paper; A.Y., R.N., T.Y., M.T., H.Y., M.R., and E.A. performed research; T.S. designed research; J.F.L., N.T.T., and T.M. designed research and wrote the paper; and O.G.O. collected samples and performed research.

Conflict-of-interest disclosure: M.S.S., M.R., T.S., J.F.L., and N.T.T. are employees of Astex Therapeutics Ltd. The remaining authors declare no competing financial interests.

The current affiliation of M.R. is KGaA Germany, Merck Serono Research, Darmstadt, Germany.

Correspondence: Shinya Kimura, Division of Hematology, Respiratory Medicine and Oncology, Department of Internal Medicine, Faculty of Medicine, Saga University, 5-1-1 Nabeshima, Saga 849-8501, Japan; e-mail: shkimu@kuhp.kyoto-u.ac.jp.

References

1. Goldman JM, Melo JV. Chronic myeloid leukemia-advances in biology and new approaches to treatment. *N Engl J Med.* 2003;349(15):1451-1464.
2. Druker BJ, Sawyers CL, Kantarjian H, et al. Activity of a specific inhibitor of the BCR-ABL tyrosine kinase in the blast crisis of chronic myeloid leukemia and acute lymphoblastic leukemia with the Philadelphia chromosome. *N Engl J Med.* 2001; 344(14):1038-1042.
3. Ottmann OG, Druker BJ, Sawyers CL, et al. A phase 2 study of imatinib in patients with relapsed or refractory Philadelphia chromosome-positive acute lymphoid leukemias. *Blood.* 2002;100(6): 1965-1971.
4. Gorre ME, Mohammed M, Ellwood K, et al. Clinical resistance to STI-571 cancer therapy caused by BCR-ABL gene mutation or amplification. *Science.* 2001;293(5531):876-880.
5. Nardi V, Azam M, Daley GQ. Mechanisms and implications of imatinib resistance mutations in BCR-ABL. *Curr Opin Hematol.* 2004;11(1):35-43.
6. Shah NP, Tran C, Lee FY, et al. Overriding imatinib resistance with a novel ABL kinase inhibitor. *Science.* 2004;305(5682):399-401.
7. Weisberg E, Manley PW, Breitenstein W, et al. Characterization of AMN107, a selective inhibitor of native and mutant Bcr-Abl. *Cancer Cell.* 2005; 7(2):129-141.
8. Golas JM, Arndt K, Etienne C, et al. SKI-606, a 4-anilino-3-quinolinecarbonitrile dual inhibitor of Src and Abl kinases, is a potent antiproliferative agent against chronic myelogenous leukemia cells in culture and causes regression of K562 xenografts in nude mice. *Cancer Res.* 2003;63(2):375-381.
9. Kimura S, Naito H, Segawa, et al. NS-187, a potent and selective dual Bcr-Abl/Lyn tyrosine kinase inhibitor, is a novel agent for imatinib-resistant leukemia. *Blood.* 2005;106(12):3948-3954.
10. Yokota A, Kimura S, Masuda S, et al. INNO-406, a novel BCR-ABL/Lyn dual tyrosine kinase inhibitor, suppresses the growth of Ph$^+$ leukemia cells in the central nervous system, and cyclosporine A augments its in vivo activity. *Blood.* 2007;109(1): 306-314.
11. Bradeen HA, Eide CA, O'Hare T, et al. Comparison of imatinib mesylate, dasatinib (BMS-354825), and nilotinib (AMN107) in an N-ethyl-N-nitrosourea (ENU)-based mutagenesis screen: high efficacy of drug combinations. *Blood.* 2006;108(7):2332-2338.
12. Deguchi Y, Kimura S, Ashihara E, et al. Comparison of imatinib, dasatinib, nilotinib and INNO-406 in imatinib-resistant cell lines. *Leuk Res.* 2008; 32(6):980-983.
13. Tanaka R, Kimura S. Abl tyrosine kinase inhibitors for overriding Bcr-Abl/T315I: from the second to third generation. *Expert Rev Anticancer Ther.* 2008;8(9):1387-1398.
14. Keen N, Taylor S. Aurora-kinase inhibitors as anticancer agents. *Nat Rev Cancer.* 2004;4(12):927-936.
15. Marumoto T, Zhang D, Saya H. Aurora-A–a guardian of poles. *Nat Rev Cancer.* 2005;5(1):42-50.
16. Carvajal RD, Tse A, Schwartz GK. Aurora kinases: new targets for cancer therapy. *Clin Cancer Res.* 2006;12(23):6869-6875.
17. Katayama H, Brinkley WR, Sen S. The Aurora kinases: role in cell transformation and tumorigenesis. *Cancer Metast Rev.* 2003;22(4):451-464.
18. Howard S, Berdini V, Boulstridge J, et al. Fragment-based discovery of the pyrazol-4-yl urea (AT9283), a multi-targeted kinase inhibitor with potent Aurora kinase activity. *J Med Chem.* 2009; 52(2):379-388.
19. Curry J, Angove H, Fazal L, et al. Aurora B kinase inhibition in mitosis: strategies for optimising the use of aurora kinase inhibitors such as AT9283. *Cell Cycle.* 2009;8(12):1921-1929.
20. Segawa H, Kimura S, Kuroda J, et al. Zoledronate synergizes with imatinib mesylate to inhibit Ph$^+$ primary leukaemic cell growth. *Br J Haematol.* 2005;130(4):558-560.
21. Jones G, Willett P, Glen RC et al. Development and validation of a genetic algorithm for flexible docking. *J Mol Biol.* 1997;267(3):727-748.
22. Eldridge MD, Murray CW, Auton TR, et al. Empirical scoring functions, I: the development of a fast empirical scoring function to estimate the binding affinity of ligands in receptor complexes. *J Comput Aided Mol Des.* 1997;11(5):425-445.
23. Kuroda J, Kimura S, Segawa H, et al. The third-generation bisphosphonate zoledronate synergistically augments the anti-Ph$^+$ leukemia activity of imatinib mesylate. *Blood.* 2003;102(6):2229-2235.
24. Kimura S, Kuroda J, Segawa H, et al. Anti-proliferative efficacy of the third-generation bisphosphonate zoledronic acid combined with other anticancer drugs in leukemic cell lines. *Int J Hematol.* 2004;79(1):37-43.
25. Melo JV, Chuah C. Resistance to imatinib mesylate in chronic myeloid leukaemia. *Cancer Lett.* 2007;249(2):121-132.
26. Branford S. Chronic myeloid leukemia: molecular monitoring in clinical practice. *Hematology Am Soc Hematol Educ Program.* 2007;376-383.
27. Soverini S, Colarossi S, Gnani A, et al. Resistance to dasatinib in Philadelphia-positive leukemia patients and the presence or the selection of mutations at residues 315 and 317 in the BCR-ABL kinase domain. *Haematologica.* 2007;92: 401-404.
28. Nicolini FE, Hayette S, Corm S, et al. Clinical outcome of 27 imatinib mesylate-resistant chronic myelogenous leukemia patients harboring a T315I BCR-ABL mutation. *Haematologica.* 2007; 92:1238-1241.
29. Soverini S, Colarossi S, Gnani A, et al. Contribution of ABL kinase domain mutations to imatinib resistance in different subsets of Philadelphia-positive patients: by the GIMEMA Working Party on Chronic Myeloid Leukemia. *Clin Cancer Res.* 2006;12(24):7374-7379.
30. Schindler T, Bornmann W, Pellicena P, et al. Structural mechanism for STI-571 inhibition of Abelson tyrosine kinase. *Science.* 2000; 289(5486):1938-1942.
31. Corbin AS, Buchdunger E, Pascal F, Druker BJ. Analysis of the structural basis of specificity of the Abl kinase by STI571. *J Biol Chem.* 2002; 277(35):32214-32219.
32. Pricl S, Fermeglia M, Ferrone M, et al. T315I-mutated Bcr-Abl in chronic myeloid leukemia and imatinib: insights from a computational study. *Mol Cancer Ther.* 2005;4(8):1167-1174.
33. Lee TS, Potts SJ, Kantarjian H, et al. Molecular basis explanation for imatinib resistance of BCR-ABL due to T315I and P-loop mutations from molecular dynamics simulations. *Cancer.* 2008; 112(8):1744-1753.
34. Young MA, Shah NP, Chao LH, et al. Structure of the kinase domain of an imatinib-resistant Abl mutant in complex with the Aurora kinase inhibitor VX-680. *Cancer Res.* 2006;66(2):1007-1014.
35. Modugno M, Casale E, Moll J, et al. Crystal structure of the T315I Abl mutant in complex with the Aurora kinases inhibitor PHA-739358. *Cancer Res.* 2007;67(17):7987-7990.
36. Giles FJ, Cortes J, Jones D, et al. MK-0457, a novel kinase inhibitor, is active in patients with chronic myeloid leukemia or acute lymphocytic leukemia with the T315I BCR-ABL mutation. *Blood.* 2007;109(2):500-502.
37. Bebbington D, Binch H, Charrier JD, et al. The discovery of the potent aurora inhibitor MK-0457 (VX-680). *Bioorg Med Chem Lett.* 2009;19(13): 3586-3592.
38. Gontarewicz A, Balabanov S, Brummendorf TH, et al. Simultaneous targeting of Aurora kinases and Bcr-Abl kinase by the small molecule inhibitor PHA-739358 is effective against imatinib-resistant BCR-ABL mutations including T315I. *Blood.* 2008;111(8):4355-4364.
39. Shah NP, Kantarjian HM, Kim DW, et al. Intermittent target inhibition with dasatinib 100 mg once daily preserves efficacy and improves tolerability in imatinib-resistant and -intolerant chronic-phase chronic myeloid leukemia. *J Clin Oncol.* 2008; 26(19):3204-3212.
40. Shah NP, Kasap C, Weier C, et al. Transient potent BCR-ABL inhibition is sufficient to commit chronic myeloid leukemia cells irreversibly to apoptosis. *Cancer Cell.* 2008;14(6):485-493.
41. Naito H, Kimura S, Nakaya Y, et al. In vivo antiproliferative effect of NS-187, a dual Bcr-Abl/Lyn tyrosine kinase inhibitor, on leukemic cells harbouring Abl kinase domain mutations. *Leuk Res.* 2006;30(11):1443-1446.
42. Kantarjian H, le Coutre P, Cortes J, et al. Phase I study of INNO-406, a dual Abl/Lyn kinase inhibitor, in Philadelphia chromosome-positive leukemias after imatinib resistance or intolerance. *Cancer.* 2010;116(11):2665-2672.
43. Kristeleit R, Calvert H, Arkenau H, et al. Phase I study of AT9283, an aurora kinase inhibitor, in patients with refractory solid tumors. *J Clin Oncol.* 2009;27:15s.

Cancer Letters 294 (2010) 245–253

Contents lists available at ScienceDirect

Cancer Letters

journal homepage: www.elsevier.com/locate/canlet

A combination of a DNA-chimera siRNA against PLK-1 and zoledronic acid suppresses the growth of malignant mesothelioma cells *in vitro*

Eri Kawata [a,b,1], Eishi Ashihara [a,*,1], Yoko Nakagawa [a], Takahiro Kiuchi [a], Mai Ogura [a], Hisayuku Yao [a], Kazuki Sakai [a], Ruriko Tanaka [a], Rina Nagao [a], Asumi Yokota [a], Miki Takeuchi [a], Shinya Kimura [c], Hideyo Hirai [a], Taira Maekawa [a]

[a] *Department of Transfusion Medicine & Cell Therapy, Kyoto University Hospital, 54 Kawahara-cho Shogoin, Sakyo-ku, Kyoto 606-8507, Japan*
[b] *Division of Internal Medicine, Kyoto Second Red Cross Hospital, 355 Kamannza Marutamachi, Kamigyo-ku, Kyoto 602-8026, Japan*
[c] *Division of Hematology, Respiratory Medicine, and Oncology, Department of Internal Medicine, Faculty of Medicine, Saga University, 5-1-1 Nabeshima, Saga 849-8501, Japan*

ARTICLE INFO

Article history:
Received 24 November 2009
Received in revised form 6 February 2010
Accepted 10 February 2010

Keywords:
PLK-1
RNA interference
DNA-chimeric siRNA
Bisphosphonate
Malignant mesothelioma

ABSTRACT

Although novel agents effective against malignant mesothelioma (MM) have been developed, the prognosis of patients with MM is still poor. We generated a DNA-chimeric siRNA against polo-like kinase-1 (PLK-1), which was more stable in human serum than the non-chimeric siRNA. The chimeric PLK-1 siRNA inhibited MM cell proliferation through the induction of apoptosis. Next, we investigated the effects of zoledronic acid (ZOL) on MM cells, and found that ZOL also induced apoptosis in MM cells. Furthermore, ZOL augmented the inhibitory effects of the PLK-1 siRNA. In conclusion, combining a PLK-1 siRNA with ZOL treatment is an attractive strategy against MM.

1. Introduction

Malignant mesothelioma (MM) is an aggressive tumor, which develops from the mesothelial surface of the pleural and peritoneal cavities. Asbestos is well-known as a carcinogen in MM and the incidence of MM is increasing worldwide [1]. Although several surgical approaches have been proven to be effective [2,3], a combination of therapies including chemotherapeutic agents, radiation, and immunotherapy are required to fight the disease. However, in spite of the emergence of novel effective anticancer agents such as pemetrexed [4,5] and raltitrexed [6,7], the prognosis of patients with MM is still poor [8,9]. Therefore, the development of novel effective therapeutic strategies is essential to improve the prognosis of this disease.

RNA interference (RNAi) is a process involving sequence specific post-transcriptional gene silencing induced by double-stranded (ds) RNA. It is widely applied as a powerful tool in postgenomic research, and has been experimentally introduced into the field of cancer therapy. Synthetic, short interfering RNAs (siRNAs) for inducing RNAi are 19- to 21-nucleotide dsRNAs with two-nucleotide 3′ overhangs at either end [10,11]. Unfotunately, siRNAs are degraded by endogenous nucleases when administered *in vivo*. Many techniques, including the use of DNA-chimeric siRNAs, have been developed to protect siRNAs from such degradation [10,12,13]. Previous investigations have revealed that their silencing activity is as powerful as that of non-chimeric siRNAs [12–14].

Polo-like kinase-1 (PLK-1) belongs to the PLK family of serine/threonine kinases and is highly conserved among eukaryotes. PLK-1 regulates cell division at several points during the mitotic phase of the cell cycle, including: mitotic entry through CDK1 activation, bipolar spindle

* Corresponding author. Tel.: +81 75 751 3630; fax: +81 75 751 4283.
E-mail address: ash0325@kuhp.kyoto-u.ac.jp (E. Ashihara).
[1] These authors contribute equal to this work.

0304-3835/$ - see front matter © 2010 Elsevier Ireland Ltd. All rights reserved.
doi:10.1016/j.canlet.2010.02.008

formation, chromosome alignment, segregation of chromosomes, and cytokinesis [15,16]. Previous studies have reported that PLK-1 is overexpressed in cancerous tissues and that PLK-1 expression levels are tightly correlated with histological grades of tumors, clinical stages, and the patients' prognosis [17–20]. Thus, PLK-1 is considered to be a suitable target for cancer therapy, and several small molecular targeting agents have been used in clinical trials [21,22], while siRNAs against PLK-1 have been investigated in preclinical studies [19,20,23].

Bisphosphonates (BPs) are inhibitors of bone-resorption, and second- and third-generation BPs have been developed primarily to treat benign and malignant bone disease [24]. This class of drugs inhibits the proliferation of cancer cells by preventing the post-translational prenylation of small GTPases including the Ras family proteins [25]. We have demonstrated previously that third-generation BPs such as zoledronic acid (ZOL) and minodronic acid (YM529) have direct anti-tumor effects against different cancer cells [26–30].

In the present study, we have investigated the effects of a DNA-chimeric PLK-1 siRNA and ZOL on MM cells *in vitro*. Our results show that these agents induce apoptosis and inhibit the proliferation of MM cells. In addition, we found that ZOL enhances the inhibitory effects of the PLK-1 siRNA.

2. Materials and methods

2.1. Cell lines, reagents, and animals

The human MM cell lines H2452, H2052, H28, and 211H were cultured in RPMI1640 medium (Gibco, Tokyo, Japan) containing 10% heat-inactivated fetal calf serum (FCS; Invitrogen, Tokyo, Japan), *l*-glutamine (Gibco), and 1% penicillin–streptomycin (Gibco). The normal human dermal fibroblast (NHDF) cells were cultured in Dulbecco's Modified Eagle medium (DMEM; Gibco) containing 10% FCS, *l*-glutamine, and 1% penicillin–streptomycin. All cell lines were maintained at 37 °C in a fully humidified atmosphere of 5% CO_2 in air. All four MM cell lines were obtained from the American Type Culture Collection (Rockville, MD). Normal fibroblast NHDF cells were purchased from Kurabo (Osaka, Japan). LIC™ Transfection Reagent (Hayashi Kasei, Tokyo, Japan) was used for transfection into MM cells. ZOL (1-hydroxy-2-[1*H*-imidazole-1-yl]ethylidene-bisphosphonic acid) was obtained from Novalits Pharma AG (Basel, Switzerland).

We generated two types of siRNA against PLK-1 (GenBank accession number NM_005030) using siDIRECT™ (alphaGEN Co, Ltd, Tokyo, Japan). One of the siRNAs contained of ribonucleotides and the other was a DNA-chimeric siRNA consisting partially of deoxyribonucleotides. The oligonucleotide sequences of the non-chimeric PLK-1 siRNA against PLK-1 were: sense strands, 5′- GCACCGAAACCG AGUUAUUCA-3′ and that antisense strand, 5′-AAUAACUC GGUUUCGGUGCAG-3′. The sequences of the DNA-chimeric siRNA against PLK-1 were: sense strand, 5′-GCACCGAAAC CGAgttattca-3′, and antisense strand, 5′-aataacUCGGUUU CGGUGCAG-3′. This DNA-modified siRNA was constructed by substituting six ribonucleotides at the 5′ end of the guide strand and the 3′ end of the passenger strand with the cognate deoxyribonucleotides (designated in lower case). The oligonucleotide sequences for the chimeric siRNA controls were: sense strand, 5′-GUACCGCACGUCAttcgtatt-3′, and antisense strand, 5′- tacgaaUGACGUGCG GUACGU-3′. The sequences for the non-chimeric control siRNA were: sense strand, 5′-GUACCGCACGUCAUUC GUAUU-3′, and antisense strand, 5′-UACGAAUGACGUGCG-GUACGU-3′. All siRNAs used were chemically synthesized (Hokkaido System Science Co. Ltd., Hokkaido, Japan).

2.2. Stability of the DNA-chimera siRNA in human serum

We investigated the stability of the DNA-chimeric and non-chimeric siRNAs in human serum. Each siRNA was incubated in human serum (95%) at 37 °C. Serum RNase was inactivated by adding SDS and proteinase K, and then digested samples were loaded onto 15% polyacrylamide gel, which was then stained using SYBR Gold (Invitrogen).

2.3. Growth inhibitory effects of PLK-1 siRNA

Cell proliferation was determined by the modified MTT assay using the Cell-Counting Kit-8 (Dojindo Laboratory, Kumamoto, Japan) as previously described [19,20]. Cells were seeded in a flat-bottomed 96-well plate (Becton Dickinson, Tokyo, Japan) at 3×10^3 cells in 100 μl of medium per well and incubated with serial dilutions of the DNA-chimeric siRNA for 72 h. The mean of four samples was calculated. Half-maximal inhibition constants (IC_{50}s) were determined with the nonlinear regression program CalcuSyn (Biosoft, Cambridge, UK).

2.4. Growth inhibitory effects of zoledronic acid

Cell proliferation was determined by the modified MTT assay using the Cell-Counting Kit-8 as mentioned above. Cells were seeded in a flat-bottomed 96-well plate (Becton Dickinson, Tokyo, Japan) at 3×10^3 cells in 100 μl of medium per well and incubated with serial dilutions of ZOL for 72 h. The mean of four samples was calculated. Half-maximal inhibition constants (IC_{50}s) were determined with the nonlinear regression program CalcuSyn. We also evaluated the combined effects of concurrent PLK-1 siRNA and ZOL treatment on H2452 and H28 mesothelioma cell lines and the analyzed data is shown by the combination index (CI). CI is a method for quantifying drug cytotoxic synergism based on the mass-action law principle derived from enzyme kinetic models. This method was developed by Chou and Talalay [31,32] which has been widely used to evaluate interactions of antineoplastic agents [33–36]. Cells were incubated for 72 h with six concentrations (0.25, 0.5, 0.75, 1.0, 1.5, or 2.0 times the IC_{50}) of each agent or both in combination using the constant ratio design followed by the modified MTT assay. We calculated the combination indexes (CIs) as reported previously [33–36], and calculated the fraction affected (Fa) at each dilution (for example, Fa of 0.25 equals 75% viable cells). This method provides a quantification of the synergism ($CI < 1$), additive effect

(CI = 1), and antagonism (CI > 1) at different dose and effect levels [31]. Calculations of the CI were made under the assumption that the mechanisms of action of the evaluated drugs were not mutually exclusive.

2.5. Cell cycle and apoptosis analysis

Cell cycle analysis using propidium iodide (PI) was performed as previously described [20]. Apoptosis induced by each siRNA treatment or ZOL treatment was determined using the Annexin-V-FITC Apoptosis Detection Kit I (BD Pharmingen, San Jose, CA) as recommended by the manufacturer. Cells were analyzed with FACS CANTO II using Diva software (BD Bioscience).

2.6. Western blotting analysis

Following the transfection of cells with PLK-1 siRNA, or treatment with ZOL, as described above, the medium was aspirated and the cells were washed with ice-cold PBS (−). The cells were lysed with ice-cold RIPA buffer (50 mM Tris–HCl [pH 7.4], 0.25 M NaCl, 5 mM EDTA, 20 mM NaF, 1% NP-40) with PMSF (1 mM) and protease inhibitor (10 μg/ml). The cells were then scraped off the plate, and the suspension of cells in lysis buffer was transferred to a centrifuge tube, which was placed on ice for 15 min with an occasional vortex to ensure complete lysis. The cell suspension was then cleared by centrifugation at 14,000g for 30 min at 4 °C, and the supernatant (total cell lysis) was either used immediately or stored at −80 °C. The protein concentration was determined using the DC Protein Assay (Bio-Rad Laboratories, Osaka, Japan).

Immunoblotting was performed as previously described [20]. The following primary antibodies (Abs) were used: rabbit polyclonal anti-PLK-1 Ab (Upstate Biotechnology Inc., Charlottesville, VA); rabbit polyclonal anti-caspase-3 Ab; rabbit polyclonal anti-cleaved caspase-3 Ab (Cell Signaling Technology, Danvers, MA); polyclonal anti-Rap1A Ab (Santa Cruz Biotechnology, Santa Cruz, CA); mouse monoclonal anti-RhoA Ab (Santa Cruz Biotechnology); mouse monoclonal anti-Ras Ab (BD Bioscience), and rabbit polyclonal anti-actin Ab (Sigma–Aldrich, Tokyo, Japan).

3. Results

3.1. Stability of the DNA-chimera siRNA in human serum

An siRNA can be protected from RNase or nuclease cleavage by the partial substitution of ribonucleotides with deoxyribonucleotides at the 5′ end of the guide strand and the 3′ end of the passenger strand. Therefore, we first designed the PLK-1 siRNA using siDIRECT™ and then converted this siRNA into a DNA-chimeric siRNA. We incubated the DNA-chimeric, or non-chimeric siRNAs against PLK-1 in 95% human serum and investigated their degeneration. The non-chimeric siRNA degenerated in a time-dependent manner, while the DNA-chimeric siRNA did not degenerate for at least 120 min (Fig. 1A). This result shows that the chimeric siRNA is more stable in human serum than the non-chimeric siRNA.

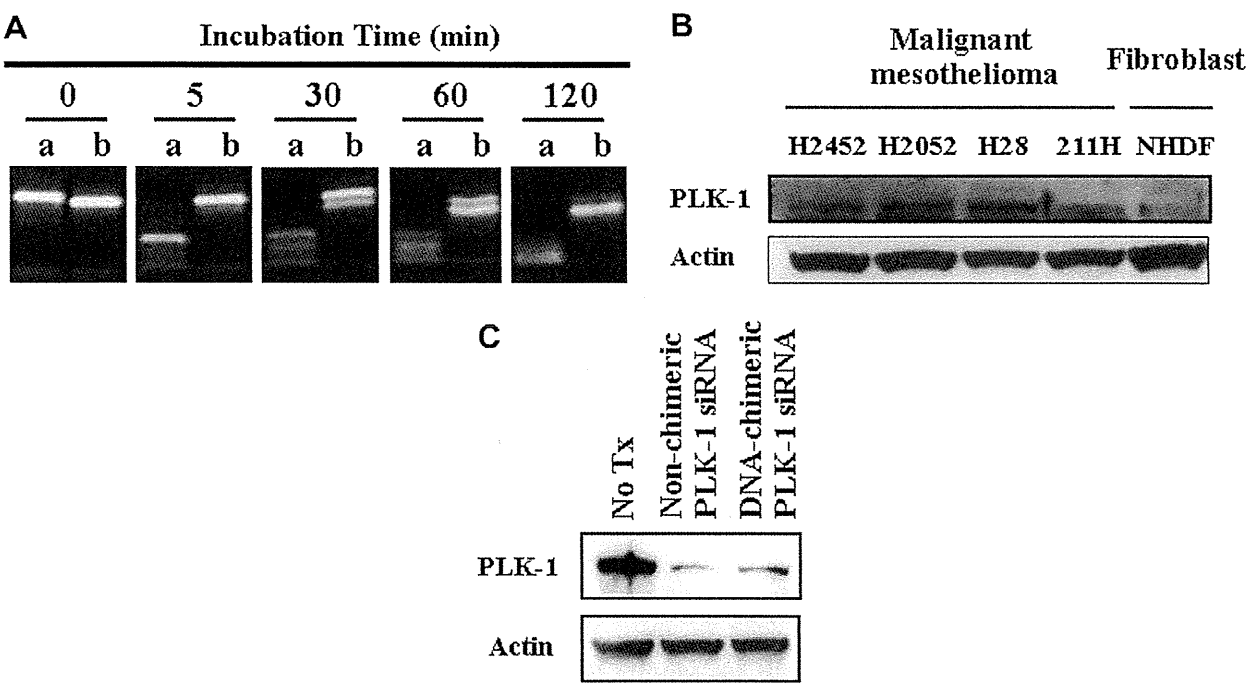

Fig. 1. DNA-chimeric siRNA against PLK-1 is more stable in human serum than a non-chimeric siRNA. (A) Each siRNA was incubated in human serum (95%) at 37 °C. Serum RNase was inactivated by adding SDS and proteinase K, and then digested samples were loaded onto a 15% polyacrylamide gel. The gel was stained by SYBR Gold. (a): non-chimeric PLK-1 siRNA, (b): DNA-chimeric PLK-1 siRNA. (B) PLK-1 expression in MM cells. Immunoblotting of whole cell lysates obtained from MM cell lines and normal NHDF human fibroblast cells. (C) Depletion of PLK-1 expression in H2452 MM cells in response to treatment with non-chimeric or DNA-chimeric PLK-1 siRNA. We obtained whole cell lysetas from H2452 MM cells 72 h after the transfection of non-chimeric or DNA-chimeric PLK-1 siRNA (50 nM), and immunoblotting was performed as described in Section 2.

3.2. DNA-chimeric PLK-1 siRNA inhibited the growth of mesothelioma cells

We examined the PLK-1 expression in four MM cell lines: H2452, H2042, H28, and 211H cell lines. All cell lines examined expressed a higher level of PLK-1 than normal NHDF fibroblast cells (Fig. 1B). Next we confirmed the knockdown effects of both DNA-chimeric and non-chimeric PLK-1 siRNAs in MM cells. We transfected both types of siRNAs into H2452 MM cells, and both siRNAs effectively knocked down PLK-1 expression (Fig. 1C). Then we investigated the inhibitory effects of the DNA-chimeric PLK-1 siRNA on MM cells *in vitro*. Western blot analysis showed that the transfection of the DNA-chimeric PLK-1 siRNA suppressed PLK-1 expression in H2452 mesothelioma cells in a dose-dependent manner, whereas the nonsense chimeric siRNA (100 nM) did not (Fig. 2A). The IC_{50} values for H2452 and H28 cells at 72 h exposure were 1.6 nM and 38.7 nM, respectively. Out next step was to examine the growth inhibitory effects of the DNA-chimeric siRNA against PLK-1 on H2452 and H28 mesothelioma cells using a modified MTT assay. As shown in Fig. 2B, the chimeric PLK-1 siRNA inhibited cell growth in a dose-dependent manner, whereas no significant inhibitory effects were detected in normal NHDF cells (Fig. 2C).

3.3. The mechanisms of cell death induced by PLK-1 depletion

Next we investigated the mechanisms of cell death caused by PLK-1 siRNA transfection. Cell cycle analysis confirmed that PLK-1 siRNA treatment induced G2/M arrest as previously reported [19,20], and revealed an increase in the subG1 fraction 72 h after transfection with the DNA-chimeric PLK-1 siRNA (Fig. 3A, upper panel). Early apoptotic cells (Annexin – V+/PI – fraction), and late apoptotic cells and necrotic cells

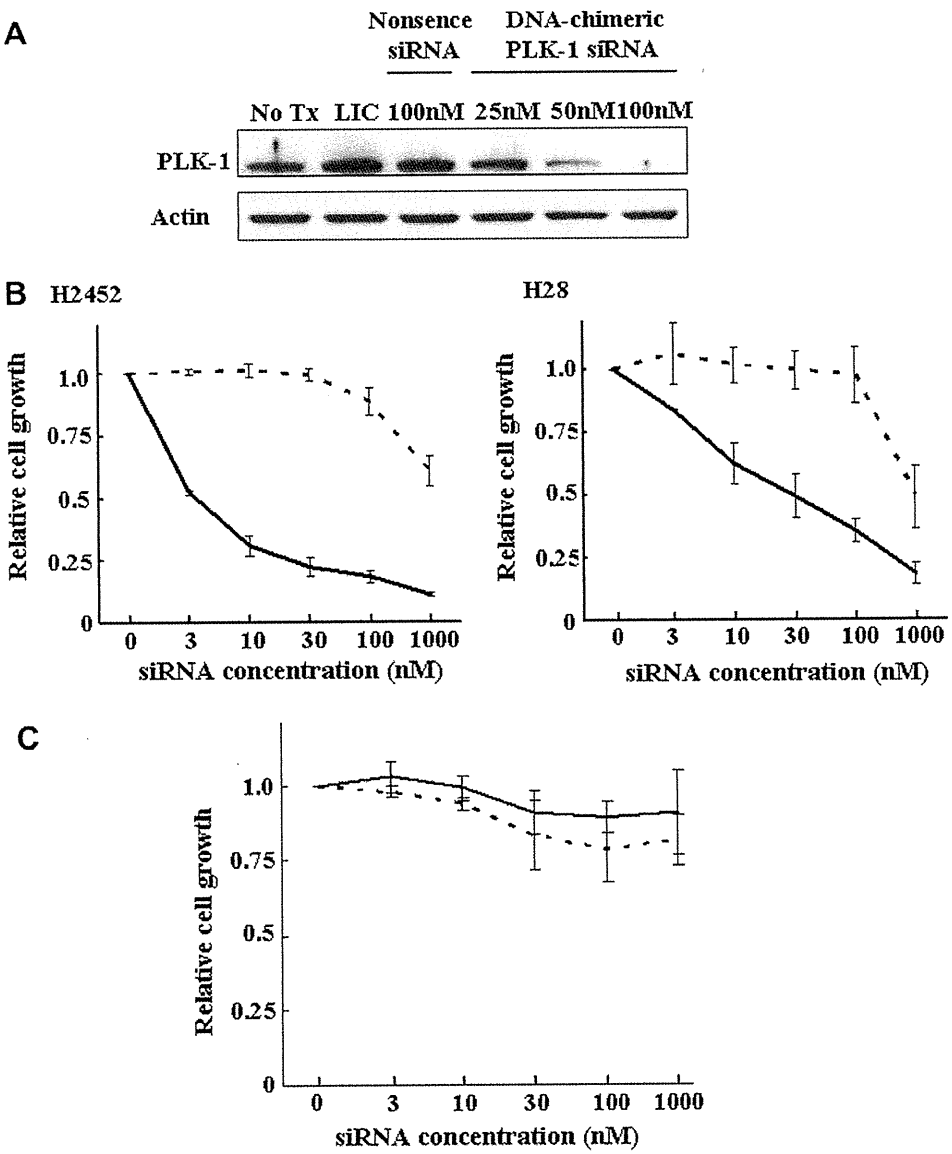

Fig. 2. DNA-chimeric PLK-1 siRNA inhibits the proliferation of MM cells, but not NHDF normal fibroblast cells. (A) Expression of PLK-1 in H2452 MM cell lines. H2452 cells were incubated with serial dilutions of DNA-chimeric PLK-1 siRNA and LIC transfection reagent for 72 h. Whole cell lysates were obtained and immunoblotting was performed as described in Section 2. (B) Cell proliferation was determined by the modified MTT assay as described in Section 2. DNA-chimeric PLK-1 siRNA shows inhibitory growth effects on H2452 and H28 MM cells in a dose-dependent manner. (C) DNA-chimeric PLK-1 siRNA does not inhibit the proliferation of normal NHDF fibroblast cells. Data represents the means ± standard deviations (SD) of three independent experiments. Solid and dotted lines indicate chimeric PLK-1 siRNA and chimeric control siRNA, respectively.

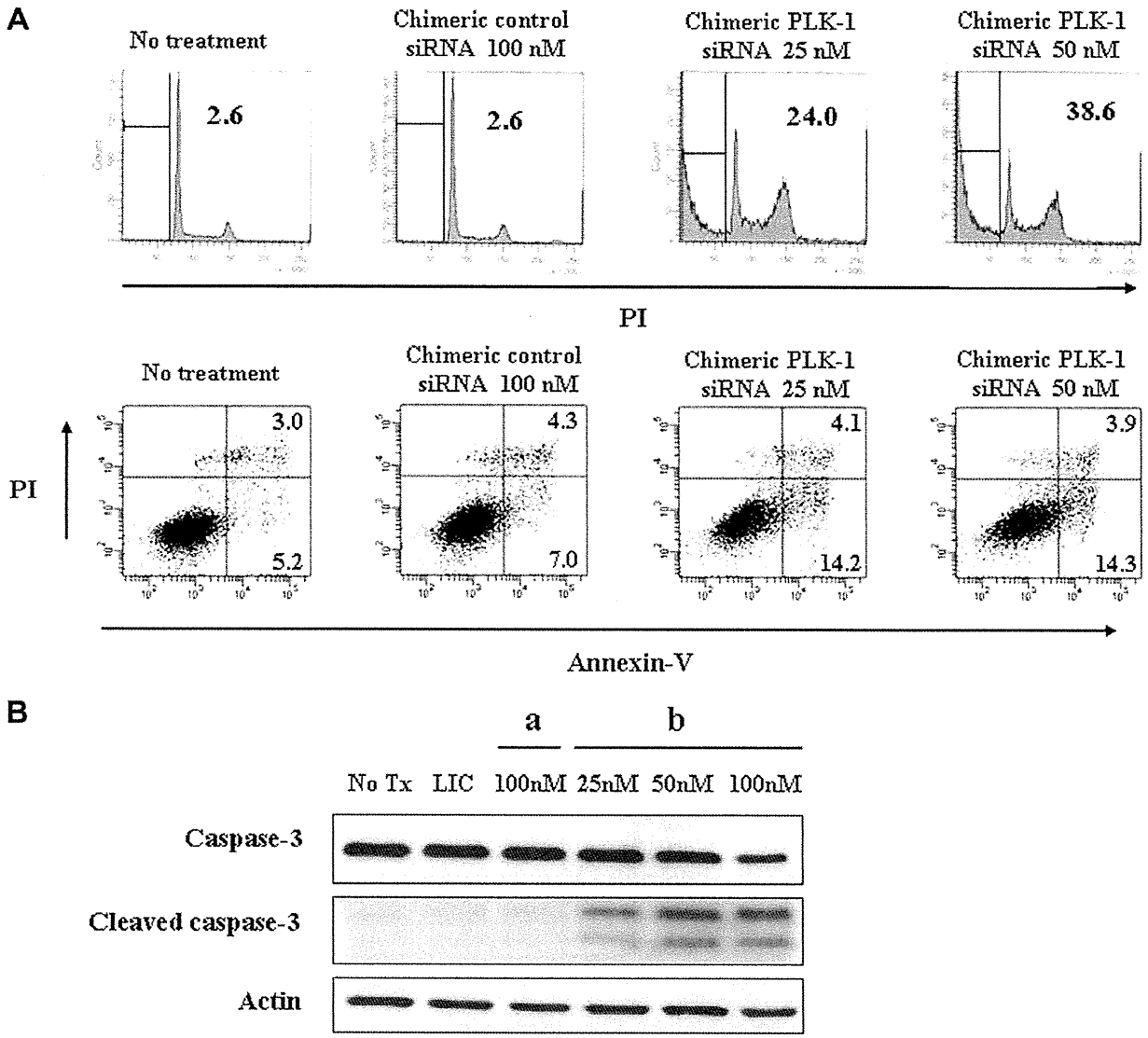

Fig. 3. DNA-chimeric PLK-1 siRNA treatment induces apoptosis in H2452 MM cells by activating caspase-3. (A: upper panels) Cell cycle analysis in H2454 MM cells using propidium iodide (PI) was performed after 72 h of treatment with the chimeric control, or chimeric PLK-1 siRNAs, at the concentration indicated. Results are representative of three independent experiments. The numbers inside each histogram indicate the percentage of the subG1 fraction. (A: lower panels) Determination of apoptosis induced by each siRNA treatment. Results are representative of three independent experiments. The numbers inside each quadrant indicate the percentage of the cell population with the quadrant characteristic. (B) Cleavage of caspase-3 by DNA-chimeric PLK-1 siRNA treatment. H2452 cells were incubated with serial dilutions of DNA-chimeric PLK-1 siRNA and LIC transfection reagent for 72 h. Whole cell lysates were obtained and immunoblotting was performed as described in Section 2. (a): chimeric control siRNA, (b): chimeric PLK-1 siRNA.

(Annexin – V+/PI + fraction) also increased after DNA-chimeric PLK-1 siRNA transfection (Fig. 3A, lower panel). In addition, Western blotting analysis demonstrated an increase in cleaved caspase-3 activity following PLK-1 siRNA transfection (Fig. 3B). Thus, transfection with a PLK-1 siRNA transfection resulted in the induction of apoptosis in mesothelioma cells through the activation of caspase-3.

3.4. ZOL inhibits the growth of mesothelioma cells and synergistically augments with the effects of the PLK-1 siRNA

We examined the inhibitory effects of ZOL on H2452 and H28 mesothelioma cells using a modified MTT assay. ZOL inhibited cell growth in a dose-dependent manner, and the IC_{50} values for H2452 and H28 cells at 72 h exposures were 11.4 μM and 58.1 μM, respectively (Fig. 4A). ZOL treatment increased the subG1 fractions (Fig. 4B) and the number of apoptotic cells (Fig. 4C) in a dose-dependent manner. Furthermore, we found that caspase-3 was cleaved by ZOL treatment (Fig. 5A).

Next we investigated the unprenylation of Rap1A, RhoA, and Ras proteins. MM cell lysates were analyzed by Western blotting using Abs against Ras and the unprenylated form of Rap1A and RhoA. ZOL treatment resulted in an increase in unprenylated Rap1A and RhoA in MM cells (Fig. 5B). The anti-Ras Ab recognizes both a slower migrating band, representing the unprenylated Ras, and a faster migrating band representing the prenylated Ras [37]. After ZOL treatment, there was an increase in the unprenylated form of Ras in MM cells which was accompanied by a reduction in the prenylated form (Fig. 5B). Taken together, the results indicate that ZOL treatment induced apoptosis through the cleavage of caspase by blocking the prenylation of small GTP-binding proteins, which resulted in the inhibition of cell growth of MM cells.

We then investigated the combined effects of ZOL treatment with the PLK-1 siRNA on H2452 and H28 MM cells. PLK-1 regulates RhoA in the mitotic phase [38,39]. The modified MTT assay with six concentrations (0.25, 0.5, 0.75, 1.0, 1.5, or 2.0 times the IC_{50}) of each agent or both in combination with the constant ratio was carried out. The values of the

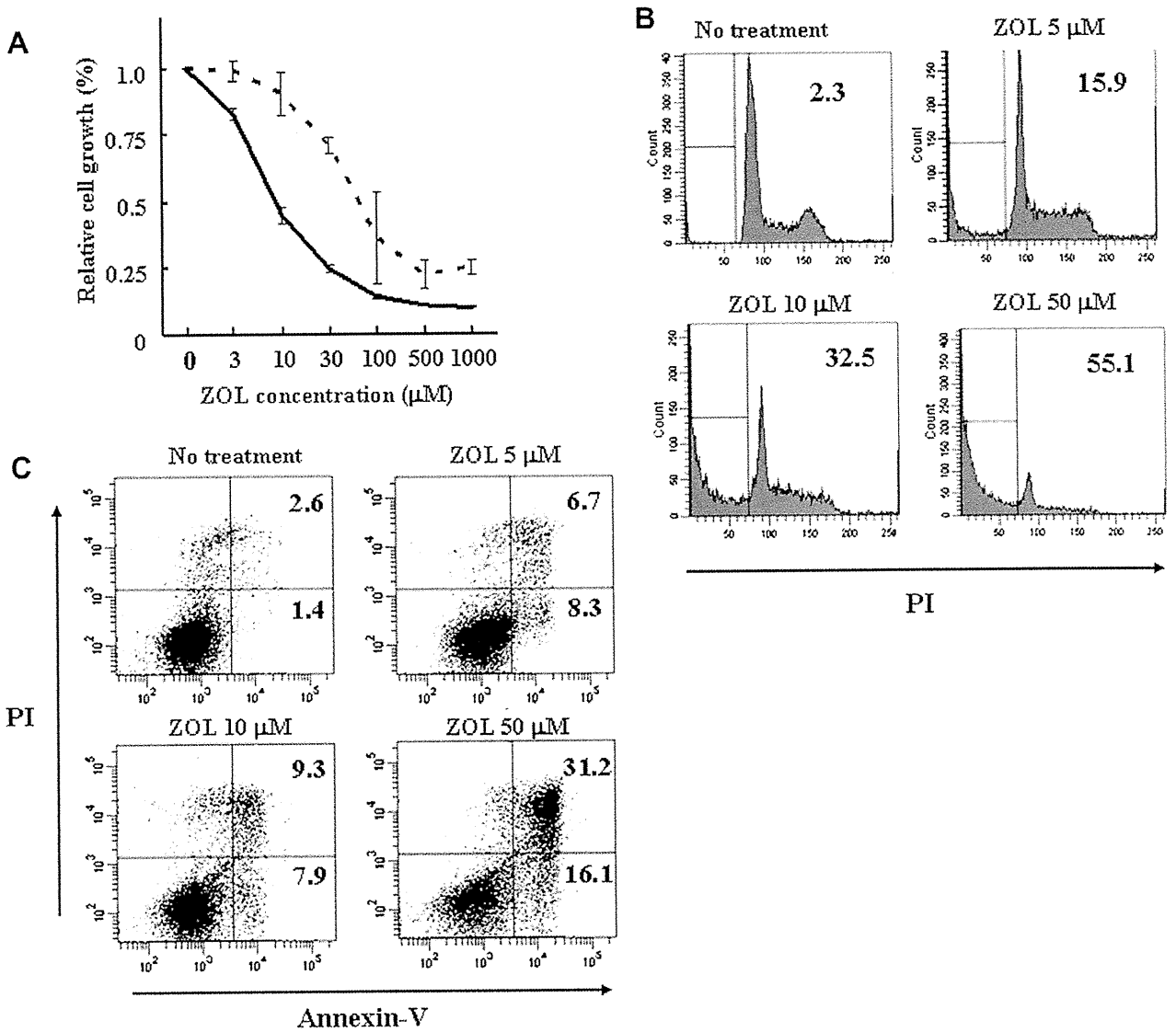

Fig. 4. ZOL treatment inhibits the proliferation of MM cells. (A) Cell proliferation was determined by the modified MTT assay as described in Section 2. ZOL treatment produced growth inhibitory effects in H2452 (solid line) and H28 (dotted line) MM cells in a dose-dependent manner. (B) Cell cycle analysis in H2452 MM cells using propidium iodide (PI) was performed after 72 h treatment with ZOL at the concentration indicated. Results are representative of three independent experiments. The numbers inside each histogram indicate the percentage of the subG1 fraction. (C) Determination of apoptosis induced by ZOL treatment at each concentration. Results are representative of three independent experiments. The numbers inside each quadrant indicate the percentage of the cell population with the quadrant characteristic.

IC_{50} which were obtained from the experiments above were used. We calculated the CIs and the Fa values at each dilution using the CalcuSyn soft as reported previously [33–36]. Dose-effect and CI–Fa plots illustrating the effects of PLK-1 siRNA and ZOL combinations are shown in Fig. 5C. As shown in the left panel of Fig. 5C, the treatment of PLK-1 siRNA combined with ZOL produced more growth inhibition than the treatments of each agent alone that are shown in Figs. 2B and 4A. The mathematically analyzed data of CI-Fa plots are shown in the right panel of Fig. 5C. In H2452 cells, the CI values at Fa 0.5, and 0.8 were 0.809 and 0.974, respectively; and in H28 cells, the CI values at Fa 0.5, and 0.8 were 0.082 and 0.836, respectively. These observations indicate that exposure to ZOL and the DNA-chimeric PLK-1 siRNA produced a synergistic effect on H2452 and H28 MM cell lines. We also investigated the alternation of the unprenylated RhoA expression in H2452 and H28 cells by the treatment of PLK-1 siRNA and ZOL. The combined treatment of concurrent PLK-1 siRNA and ZOL did not alter the unprenylated RhoA expression compared to the treatment of ZOL alone (Supplementary Fig. S1), suggesting that PLK-1 siRNA does not act on the prenylation of RhoA GTPase although PLK-1 siRNA diminishes PLK-1 expression.

4. Discussion

Synthetic siRNAs form complexes with liposomes, after which, the siRNA/liposome complex binds to the cell membrane and enters the cytoplasm via endocytosis. The complex then escapes from the endosome and releases its siRNA to the RNAi machinery [11,40]. Although single-stranded (ss) nucleic acids are rapidly degraded in serum or inside cells, ds nucleic acids are more stable than their

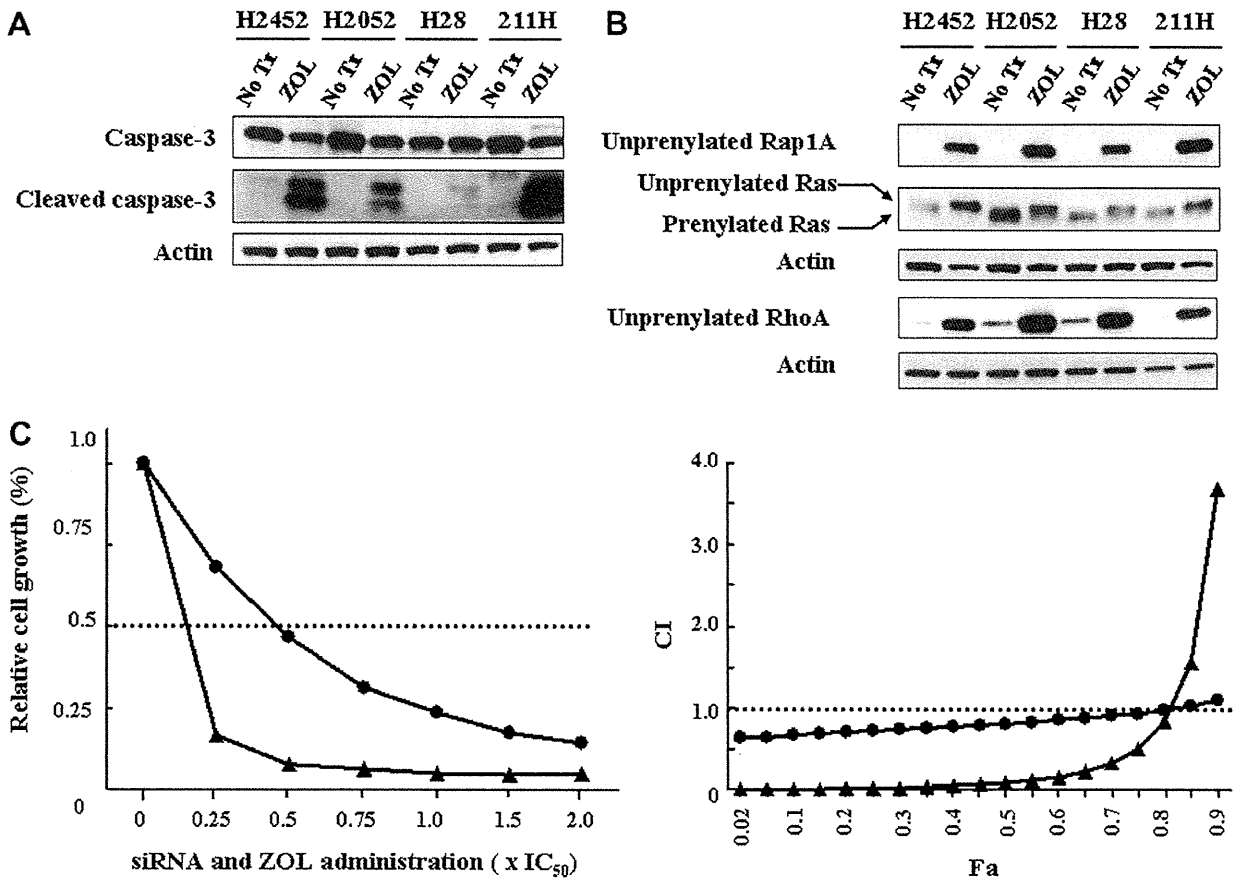

Fig. 5. Induction of apoptosis in MM cells by ZOL treatment (A and B) and combined effects of chimeric PLK-1 siRNA with ZOL. (A) Cleavage of caspase-3 by ZOL treatment. Four MM cell lines were incubated with ZOL at 50 μM for 72 h. Whole cell lysates were obtained and immunoblotting was performed as described in Section 2. (B) Evaluation of the inhibition of small GTPase protein prenylation by ZOL treatment (50 μM). Immunoblotting and immunoprecipitation were performed as described in Section 2. (C) Evaluation of the combined effects of DNA-chimeric PLK-1 siRNA and ZOL treatment on H2452 (filled circles) and H28 (filled triangles) mesothelioma cell lines. Cells were incubated for 72 h with six concentrations (0.25, 0.5, 0.75, 1.0, 1.5, or 2.0 times the IC_{50}) of each agent or both in combination using the constant ratio design followed by the modified MTT assay as described in Section 2. The IC_{50} values of PLK-1 siRNA for H2452 cells and H28 cells were 1.6 nM and 38.7 nM, respectively, and those of ZOL were 11.4 μM and 58.1 μM, respectively. Left panel: The killing curves of the concurrent administration of PLK-1 siRNA and ZOL. Right panel: Combination index (CI)-fraction affected (Fa) plots. Combination indexes were determined with the nonlinear regression program CalcuSyn.

ss counterparts; however, ds nucleic acids, including siRNAs, are still degraded and must be protected from endogenous nucleases in the bloodstream. Degradation can be avoided by the use of a suitable delivery system or by the nuclease-resistant chemical modification of the siRNA [10]. One approach involves the modification of the 2′-position of the ribose of the siRNA. Sugar modifications such as 2′-*O*-methylation, 2′-*O*-methoxyethylation, and 2′-fluoro-2′-deoxynucleoside modification can improve nuclease resistance [41,42]. Another approach involves the replacement of certain siRNA ribonucleotides with their deoxyribonucleotide counterparts.

We generated a DNA-chimeric siRNA, and substituted six basepairs from the 5′ end of the guide strand with their deoxyribonucleotide counterparts. This DNA-chimeric siRNA was more stable in human serum than the non-chimeric siRNA and showed resistance to endogenous nucleases. Moreover, the chimeric siRNA against PLK-1 decreased PLK-1 expression almost as effectively as the non-chimeric siRNA, and inhibited the proliferation of MM cells through the induction of apoptosis by cleaving caspase-3. These anti-neoplastic effects in the present study are consistent with our previous reports [19,20]. PLK-1 is overexpressed in MM cells compared to normal fibroblasts and, therefore, PLK-1 is a novel target that inhibits the proliferation of MM cells. Ui-Tei et al. [13] also demonstrated that DNA-chimeric siRNAs, in which the eight ribonucleotides from the 5′ end of the guide strand were substituted with deoxyribonucleotides, effectively induced gene-silencing without exerting the off-target effects. Our findings, taken together with the Ui-Tei's report, demonstrate that DNA-chimeric siRNAs result in safe and more effective gene-silencing and that the DNA-chimeric siRNA is much suitable for an *in vivo* administration. Further studies are warranted to evaluate the therapeutic potential of the DNA-chimeric siRNA *in vivo*.

ZOL, a third-generation BP, inhibits the activity of farnesyl diphosphate synthase in the mevalonate pathway, resulting in inhibition of the prenylation of small GTPases

[24,25]. The prenylated small GTPases including Ras, Rap-1, and Rho proteins transduce signals downstream for cell functions such as cell proliferation, adhesion, and migration [43–45], while the inhibition of these small GTPase prenylation by BPs results in the suppression of cancer progression [26–30,46–48]. In the present study, we have revealed that ZOL also inhibits the proliferation of MM cells. Treatment of MM cells with ZOL inhibited the prenylation of Rap-1A, Ras, and RhoA proteins, and induced apoptosis by cleaving capsase-3. Other investigators have also reported that ZOL inhibits the proliferation of MM cells [49,50]. Interestingly, one report demonstrated that Ca^{2+} regulates the growth inhibitory effects of BPs on MM cells [49]. Calcification is a well-known feature in MM [51,52], and BPs accumulate rapidly in bone [24,25]. We have demonstrated previously that ZOL has anti-tumor effects against osteosarcoma [29,46]. These findings collectively suggest that malignancies with ossifying features, including MM and breast cancers [48], are suitable candidates for ZOL treatment.

PLK-1 regulates cell division at several points during the mitotic phase, and RhoA is also implicated in the regulation of cytokinesis. Prenylated Rho proteins are delivered to the plasma membrane and are concentrated at the cleavage furrow of the cell during the M phase of cell cycle [53,54]. PLK-1 regulates the local activation of RhoA to promote cytokinesis [38,39] and, therefore, we hypothesized that ZOL treatment would augment the cytotoxic efficacy of the PLK-1 siRNA in MM cells. The combined ZOL and PLK-1 siRNA treatment showed synergistic effects at both low (Fa 0.5) and high (Fa 0.8) concentrations.

In conclusion, a DNA-chimeric PLK-1 siRNA inhibited cellular proliferation and induced apoptosis in MM cells, and a combination of PLK-1 siRNA and ZOL treatment revealed synergistic inhibitory effects on MM cells. The observation reported in the present study indicates that PLK-1 is a novel target for the treatment of MM and that the DNA-chimeric siRNA against PLK-1 combined with ZOL treatment would be an attractive strategy in the fight against this aggressive disease.

Conflicts of interest

All authors declare that they have no conflicts of interest.

Acknowledgements

The authors thank Naoko Hashimoto for her excellent technical assistance. The authors also thank alphaGEN Co, Ltd (Tokyo, Japan) for designing DNA-chimeric siRNAs. The authors declare that they have no commercial affiliations. This work was partly supported by Research for Promoting Technological Seeds, Japan Science and Technology Agency, by a Grant-in-Aid for Scientific Research from the Ministry of Education, Culture, Sports, Science and Technology of Japan, and by the Kobayashi Institute for Innovative Cancer Chemotherapy.

Appendix A. Supplementary material

Supplementary data associated with this article can be found, in the online version, at doi:10.1016/j.canlet.2010.02.008.

References

[1] B.W. Robinson, R.A. Lake, Advances in malignant mesothelioma, New Engl. J. Med. 353 (2005) 1591–1603.
[2] J.C. Halstead, E. Lim, R.M. Venkateswaran, S.C. Charman, M. Goddard, A.J. Ritchie, Improved survival with VATS pleurectomy–decortication in advanced malignant mesothelioma, Eur. J. Surg. Oncol. 31 (2005) 314–320.
[3] D.A. Waller, Malignant mesothelioma – British surgical strategies, Lung Cancer 45 (Suppl 1) (2004) S81–S84.
[4] G. Carteni, C. Manegold, G.M. Garcia, S. Siena, C.C. Zielinski, D. Amadori, Y. Liu, J. Blatter, C. Visseren-Grul, R. Stahel, Malignant peritoneal mesothelioma – results from the international expanded access program using pemetrexed alone or in combination with a platinum agent, Lung Cancer 64 (2009) 211–218.
[5] P. Taylor, B. Castagneto, G. Dark, M. Marangolo, G.V. Scagliotti, R.J. van Klaveren, R. Labianca, M. Serke, W. Schuette, J.P. van Meerbeeck, D. Heigener, Y. Liu, S. Adachi, J. Blatter, J. von Pawel, Single-agent pemetrexed for chemonaive and pretreated patients with malignant pleural mesothelioma: results of an international expanded access program, J. Thorac. Oncol. 3 (2008) 764–771.
[6] P. Baas, A. Ardizzoni, F. Grossi, K. Nackaerts, G. Numico, E. Van Marck, M. van de Vijver, F. Monetti, M.J. Smid-Geirnaerdt, N. van Zandwijk, C. Debruyne, C. Legrand, G. Giaccone, The activity of raltitrexed (Tomudex) in malignant pleural mesothelioma: an EORTC phase II study (08992), Eur. J. Cancer 39 (2003) 353–357.
[7] J.P. van Meerbeeck, R. Gaafar, C. Manegold, R.J. Van Klaveren, E.A. Van Marck, M. Vincent, C. Legrand, A. Bottomley, C. Debruyne, G. Giaccone, Randomized phase III study of cisplatin with or without raltitrexed in patients with malignant pleural mesothelioma: an intergroup study of the European Organisation for Research and Treatment of Cancer Lung Cancer Group and the National Cancer Institute of Canada, J. Clin. Oncol. 23 (2005) 6881–6889.
[8] C.W. Lee, N. Murray, H. Anderson, S.C. Rao, W. Bishop, Outcomes with first-line platinum-based combination chemotherapy for malignant pleural mesothelioma: a review of practice in British Columbia, Lung Cancer 64 (2009) 308–313.
[9] Y. Aelony, Raltitrexed and pemetrexed studies in mesothelioma have not shown improved quality of life nor prolonged survival compared with effective pleurodesis with thoracoscopic talc poudrage, J. Clin. Oncol. 24 (2006) 4667 (author reply 4667–4668).
[10] D. Bumcrot, M. Manoharan, V. Koteliansky, D.W. Sah, RNAi therapeutics: a potential new class of pharmaceutical drugs, Nat. Chem. Biol. 2 (2006) 711–719.
[11] E. Ashihara, E. Kawata, T. Maekawa, Future prospect of RNA interference for cancer therapies, Curr. Drug Targets. in press.
[12] A. Boutla, C. Delidakis, I. Livadaras, M. Tsagris, M. Tabler, Short 5′-phosphorylated double-stranded RNAs induce RNA interference in Drosophila, Curr. Biol. 11 (2001) 1776–1780.
[13] K. Ui-Tei, Y. Naito, S. Zenno, K. Nishi, K. Yamato, F. Takahashi, A. Juni, K. Saigo, Functional dissection of siRNA sequence by systematic DNA substitution: modified siRNA with a DNA seed arm is a powerful tool for mammalian gene silencing with significantly reduced off-target effect, Nucleic Acids Res. 36 (2008) 2136–2151.
[14] S.M. Elbashir, J. Martinez, A. Patkaniowska, W. Lendeckel, T. Tuschl, Functional anatomy of siRNAs for mediating efficient RNAi in Drosophila melanogaster embryo lysate, Embo. J. 20 (2001) 6877–6888.
[15] F.A. Barr, H.H. Sillje, E.A. Nigg, Polo-like kinases and the orchestration of cell division, Nat. Rev. Mol. Cell Biol. 5 (2004) 429–440.
[16] B.C. van de Weerdt, R.H. Medema, Polo-like kinases: a team in control of the division, Cell Cycle 5 (2006) 853–864.
[17] K. Strebhardt, A. Ullrich, Targeting polo-like kinase 1 for cancer therapy, Nat. Rev. Cancer 6 (2006) 321–330.
[18] N. Takai, R. Hamanaka, J. Yoshimatsu, I. Miyakawa, Polo-like kinases (Plks) and cancer, Oncogene 24 (2005) 287–291.
[19] M. Nogawa, T. Yuasa, S. Kimura, M. Tanaka, J. Kuroda, K. Sato, A. Yokota, H. Segawa, Y. Toda, S. Kageyama, T. Yoshiki, Y. Okada, T. Maekawa, Intravesical administration of small interfering RNA

targeting PLK-1 successfully prevents the growth of bladder cancer, J. Clin. Invest. 115 (2005) 978–985.
[20] E. Kawata, E. Ashihara, S. Kimura, K. Takenaka, K. Sato, R. Tanaka, A. Yokota, Y. Kamitsuji, M. Takeuchi, J. Kuroda, F. Tanaka, T. Yoshikawa, T. Maekawa, Administration of PLK-1 small interfering RNA with atelocollagen prevents the growth of liver metastases of lung cancer, Mol. Cancer Ther. 7 (2008) 2904–2912.
[21] P. Schoffski, Polo-like kinase (PLK) inhibitors in preclinical and early clinical development in oncology, Oncologist 14 (2009) 559–570.
[22] K. Mross, A. Frost, S. Steinbild, S. Hedbom, J. Rentschler, R. Kaiser, N. Rouyrre, D. Trommeshauser, C.E. Hoesl, G. Munzert, Phase I dose escalation and pharmacokinetic study of BI 2536, a novel polo-like kinase 1 inhibitor, in patients with advanced solid tumors, J. Clin. Oncol. 26 (2008) 5511–5517.
[23] B. Spankuch-Schmitt, J. Bereiter-Hahn, M. Kaufmann, K. Strebhardt, Effect of RNA silencing of polo-like kinase-1 (PLK1) on apoptosis and spindle formation in human cancer cells, J. Natl. Cancer Inst. 94 (2002) 1863–1877.
[24] T. Yuasa, S. Kimura, E. Ashihara, T. Habuchi, T. Maekawa, Zoledronic acid – a multiplicity of anti-cancer action, Curr. Med. Chem. 14 (2007) 2126–2135.
[25] J.R. Green, Bisphosphonates: preclinical review, Oncologist 9 (Suppl 4) (2004) 3–13.
[26] J. Kuroda, S. Kimura, H. Segawa, Y. Kobayashi, T. Yoshikawa, Y. Urasaki, T. Ueda, F. Enjo, H. Tokuda, O.G. Ottmann, T. Maekawa, The third-generation bisphosphonate zoledronate synergistically augments the anti-Ph+ leukemia activity of imatinib mesylate, Blood 102 (2003) 2229–2235.
[27] S. Matsumoto, S. Kimura, H. Segawa, J. Kuroda, T. Yuasa, K. Sato, M. Nogawa, F. Tanaka, T. Maekawa, H. Wada, Efficacy of the third-generation bisphosphonate, zoledronic acid alone and combined with anti-cancer agents against small cell lung cancer cell lines, Lung Cancer 47 (2005) 31–39.
[28] T. Yuasa, M. Nogawa, S. Kimura, A. Yokota, K. Sato, H. Segawa, J. Kuroda, T. Maekawa, A third-generation bisphosphonate, minodronic acid (YM529), augments the interferon alpha/beta-mediated inhibition of renal cell cancer cell growth both in vitro and in vivo, Clin. Cancer Res. 11 (2005) 853–859.
[29] N. Horie, H. Murata, Y. Nishigaki, T. Matsui, H. Segawa, M. Nogawa, T. Yuasa, S. Kimura, T. Maekawa, S. Fushiki, T. Kubo, The third-generation bisphosphonates inhibit proliferation of murine osteosarcoma cells with induction of apoptosis, Cancer Lett. 238 (2006) 111–118.
[30] K. Sato, T. Yuasa, M. Nogawa, S. Kimura, H. Segawa, A. Yokota, T. Maekawa, A third-generation bisphosphonate, minodronic acid (YM529), successfully prevented the growth of bladder cancer in vitro and in vivo, Brit. J. Cancer 95 (2006) 1354–1361.
[31] T.C. Chou, Drug combination studies and their synergy quantification using the Chou–Talalay method, Cancer Res. 70 (2010) 440–446.
[32] T.C. Chou, Theoretical basis, experimental design, and computerized simulation of synergism and antagonism in drug combination studies, Pharmacol. Rev. 58 (2006) 621–681.
[33] S. Kimura, J. Kuroda, H. Segawa, K. Sato, M. Nogawa, T. Yuasa, O.G. Ottmann, T. Maekawa, Antiproliferative efficacy of the third-generation bisphosphonate, zoledronic acid, combined with other anticancer drugs in leukemic cell lines, Int. J. Hematol. 79 (2004) 37–43.
[34] O.H. Temmink, E.K. Hoebe, K. van der Born, S.P. Ackland, M. Fukushima, G.J. Peters, Mechanism of trifluorothymidine potentiation of oxaliplatin-induced cytotoxicity to colorectal cancer cells, Brit. J. Cancer 96 (2007) 231–240.
[35] N. Keshelava, E. Davicioni, Z. Wan, L. Ji, R. Sposto, T.J. Triche, C.P. Reynolds, Histone deacetylase 1 gene expression and sensitization of multidrug-resistant neuroblastoma cell lines to cytotoxic agents by depsipeptide, J. Natl. Cancer Inst. 99 (2007) 1107–1119.
[36] S. Sei, J.K. Mussio, Q.E. Yang, K. Nagashima, R.E. Parchment, M.C. Coffey, R.H. Shoemaker, J.E. Tomaszewski, Synergistic antitumor activity of oncolytic reovirus and chemotherapeutic agents in non-small cell lung cancer cells, Mol. Cancer 8 (2009) 47.
[37] A.A. Reszka, J. Halasy-Nagy, G.A. Rodan, Nitrogen-bisphosphonates block retinoblastoma phosphorylation and cell growth by inhibiting the cholesterol biosynthetic pathway in a keratinocyte model for esophageal irritation, Mol. Pharmacol. 59 (2001) 193–202.
[38] B.N. Dai, Y. Yang, Z. Chau, M. Jhanwar-Uniyal, Polo-like kinase 1 regulates RhoA during cytokinesis exit in human cells, Cell Proliferat. 40 (2007) 550–557.
[39] M.E. Burkard, C.L. Randall, S. Larochelle, C. Zhang, K.M. Shokat, R.P. Fisher, P.V. Jallepalli, Chemical genetics reveals the requirement for polo-like kinase 1 activity in positioning RhoA and triggering cytokinesis in human cells, Proc. Natl. Acad. Sci. USA 104 (2007) 4383–4388.
[40] O. Zelphati, F.C. Szoka Jr., Mechanism of oligonucleotide release from cationic liposomes, Proc. Natl. Acad. Sci. USA 93 (1996) 11493–11498.
[41] S. Choung, Y.J. Kim, S. Kim, H.O. Park, Y.C. Choi, Chemical modification of siRNAs to improve serum stability without loss of efficacy, Biochem. Biophys. Res. Commun. 342 (2006) 919–927.
[42] M.A. Behlke, Chemical modification of siRNAs for in vivo use, Oligonucleotides 18 (2008) 305–319.
[43] W.J. Chia, B.L. Tang, Emerging roles for Rab family GTPases in human cancer, Biochim. Biophys. Acta 1795 (2009) 110–116.
[44] M. Hattori, N. Minato, Rap1 GTPase: functions, regulation, and malignancy, J. Biochem. 134 (2003) 479–484.
[45] N. Fehrenbacher, D. Bar-Sagi, M. Philips, Ras/MAPK signaling from endomembranes, Mol. Oncol. 3 (2009) 297–307.
[46] K. Koto, N. Horie, S. Kimura, H. Murata, T. Sakabe, T. Matsui, M. Watanabe, S. Adachi, T. Maekawa, S. Fushiki, T. Kubo, Clinically relevant dose of zoledronic acid inhibits spontaneous lung metastasis in a murine osteosarcoma model, Cancer Lett. 274 (2009) 271–278.
[47] S. Yano, H. Zhang, M. Hanibuchi, T. Miki, H. Goto, H. Uehara, S. Sone, Combined therapy with a new bisphosphonate, minodronate (YM529), and chemotherapy for multiple organ metastases of small cell lung cancer cells in severe combined immunodeficient mice, Clin. Cancer Res. 9 (2003) 5380–5385.
[48] T. Hiraga, P.J. Williams, A. Ueda, D. Tamura, T. Yoneda, Zoledronic acid inhibits visceral metastases in the 4T1/luc mouse breast cancer model, Clin. Cancer Res. 10 (2004) 4559–4567.
[49] M.A. Merrell, S. Wakchoure, J.M. Ilvesaro, K. Zinn, B. Gehrs, P.P. Lehenkari, K.W. Harris, K.S. Selander, Differential effects of Ca(2+) on bisphosphonate-induced growth inhibition in breast cancer and mesothelioma cells, Eur. J. Pharmacol. 559 (2007) 21–31.
[50] S. Wakchoure, M.A. Merrell, W. Aldrich, T. Millender-Swain, K.W. Harris, P. Triozzi, K.S. Selander, Bisphosphonates inhibit the growth of mesothelioma cells in vitro and in vivo, Clin. Cancer Res. 12 (2006) 2862–2868.
[51] A. Raizon, A. Schwartz, W. Hix, S.D. Rockoff, Calcification as a sign of sarcomatous degeneration of malignant pleural mesotheliomas: a new CT finding, J. Comput. Assist. Tomogr. 20 (1996) 42–44.
[52] F. Liu, P. Misra, E.P. Lunsford, J.T. Vannah, Y. Liu, R.E. Lenkinski, J.V. Frangioni, A dose- and time-controllable syngeneic animal model of breast cancer microcalcification, Breast Cancer Res. Treat. (2009).
[53] F.A. Barr, U. Gruneberg, Cytokinesis: placing and making the final cut, Cell 131 (2007) 847–860.
[54] S. Yoshida, S. Bartolini, D. Pellman, Mechanisms for concentrating Rho1 during cytokinesis, Genes Dev. 23 (2009) 810–823.

Cell Death and Differentiation (2010) 17, 1211–1220

www.nature.com/cdd

Glyoxalase-I is a novel target against Bcr-Abl$^+$ leukemic cells acquiring stem-like characteristics in a hypoxic environment

M Takeuchi[1,2], S Kimura*[,1,3], J Kuroda[4], E Ashihara[1], M Kawatani[5], H Osada[5], K Umezawa[6], E Yasui[7], M Imoto[8], T Tsuruo[9], A Yokota[1], R Tanaka[1], R Nagao[1], T Nakahata[10], Y Fujiyama[2] and T Maekawa[1]

Abl tyrosine kinase inhibitors (TKIs) such as imatinib and dasatinib are ineffective against Bcr-Abl$^+$ leukemic stem cells. Thus, the identification of novel agents that are effective in eradicating quiescent Bcr-Abl$^+$ stem cells is needed to cure leukemias caused by Bcr-Abl$^+$ cells. Human Bcr-Abl$^+$ cells engrafted in the bone marrow of immunodeficient mice survive under severe hypoxia. We generated two hypoxia-adapted (HA)-Bcr-Abl$^+$ sublines by selection in long-term hypoxic cultures (1.0% O_2). Interestingly, HA-Bcr-Abl$^+$ cells exhibited stem cell-like characteristics, including more cells in a dormant, increase of side population fraction, higher β-catenin expression, resistance to Abl TKIs, and a higher transplantation efficiency. Compared with the respective parental cells, HA-Bcr-Abl$^+$ cells had higher levels of protein and higher enzyme activity of glyoxalase-I (Glo-I), an enzyme that detoxifies methylglyoxal, a cytotoxic by-product of glycolysis. In contrast to Abl TKIs, Glo-I inhibitors were much more effective in killing HA-Bcr-Abl$^+$ cells both *in vitro* and *in vivo*. These findings indicate that Glo-I is a novel molecular target for treatment of Bcr-Abl$^+$ leukemias, and, in particular, Abl TKI-resistant quiescent Bcr-Abl$^+$ leukemic cells that have acquired stem-like characteristics in the process of adapting to a hypoxic environment.
Cell Death and Differentiation (2010) **17,** 1211–1220; doi:10.1038/cdd.2010.6; published online 5 February 2010

Chronic myeloid leukemia (CML) is a disorder of hematopoietic stem cells caused by the constitutive activation of the Bcr-Abl tyrosine kinase.[1] Treatment of CML has been drastically improved by the development of imatinib mesylate, an Abl tyrosine kinase inhibitor (TKI).[2,3] However, imatinib resistance is frequently observed, especially in patients with advanced-stage disease.[4] Second-generation Abl TKIs, such as dasatinib,[5] nilotinib[6] and INNO-406 (formerly NS-187),[7–9] potently overcome most imatinib resistance mechanisms.[10] However, whether TKI alone can kill all the cancerous cells, which is a prerequisite for curing CML, is in doubt because TKIs are much less effective against quiescent CML stem cells.[11,12]

Bone marrow (BM) is a hypoxic tissue, particularly at the epiphysis, which is distant from the BM arterial blood supply (Supplementary Figure 1).[13] In addition, leukemic cells are more hypoxic than normal cells in the BM because of cell crowding, due to accelerated cell growth, as well as the anemia that commonly accompanies the progression of leukemia.[14,15] The oxygen supply is frequently inadequate for the level of oxygen consumption in the microenvironment of rapidly proliferating cancer cells.[16] Although not identified conclusively until today, Bcr-Abl$^+$ CML stem cells are in a quiescent state in the niche. In addition, human primary leukemic cells expressing CD34 inoculated into immunodeficient mice initially populate the hypoxic epiphysial region.[17] Thus, it is likely that quiescent leukemic cells predominantly reside in and survive in a hypoxic BM environment.

Most cancer cells that have adapted to hypoxia are resistant to a variety of cell death stimuli.[18,19] A shift in energy production from aerobic to anaerobic respiration causes a number of dramatic changes in cell phenotype, including the accumulation of hypoxia-specific by-products, alterations in the cell cycle, and resistance to chemotherapeutic drugs. Given these observations, we hypothesized that adaptation to hypoxia is one of the causes of minimal residual disease in patients treated with Abl TKIs. The molecular mechanisms of adaptation to hypoxia may provide new targets for cancer-specific therapies that are effective against cells in hypoxic microenvironments.[20,21]

[1]Department of Transfusion Medicine and Cell Therapy, Kyoto University Hospital, Kyoto, Japan; [2]Division of Gastroenterology and Hematology, Department of Internal Medicine, Shiga University of Medical Science, Shiga, Japan; [3]Division of Hematology, Respiratory Medicine and Oncology, Department of Internal Medicine, Faculty of Medicine, Saga University, Saga, Japan; [4]Division of Hematology and Oncology, Department of Medicine, Kyoto Prefectural University of Medicine, Kyoto, Japan; [5]Antibiotics Laboratory, Discovery Research Institute, RIKEN, Saitama, Japan; [6]Department of Applied Chemistry, Faculty of Science and Technology, Keio University, Yokohama, Japan; [7]Department of Pharmaceutical Science, Research Institute of Pharmaceutical Sciences, Musashino University, Tokyo, Japan; [8]Department of Biosciences and Informatics, Faculty of Science and Technology, Keio University, Yokohama, Japan; [9]Cancer Chemotherapy Center, Japanese Foundation for Cancer Research, Tokyo, Japan and [10]Department of Pediatrics, Graduate School of Medicine, Kyoto University, Kyoto, Japan
*Corresponding author: S Kimura, Division of Hematology, Respiratory Medicine and Oncology, Department of Internal Medicine, Faculty of Medicine, Saga University, 5-1-1 Nabeshima, Saga 849-8501, Japan. Tel: +81 952 342 353; Fax: +81 952 342 017; E-mail: shkimu@cc.saga-u.ac.jp
Keywords: hypoxia; leukemia; stem cell; Glo-I; Abl tyrosine kinase
Abbreviations: TKI, tyrosine kinase inhibitor; CML, chronic myeloid leukemia; BM, bone marrow; HA, hypoxia-adapted; Glo-I, glyoxalase-I; NOG, NOD/SCID/γ_c^{null}; BBGC, *S-p*-bromobenzyl glutathione cyclopentyl diester; COTC, 2-crotonyloxymethyl-4,5,6-trihydroxycylohex-2-enone; $\Delta\psi$m, mitochondrial transmembrane potential; $DiOC_6$, 3,3′-dihexyloxacarbocyanine iodide; ECL, enhanced chemiluminescence; PMSF, phenylmethylsulfonyl fluoride; PI, propidium iodide; PB, peripheral blood
Received 30.4.09; revised 18.12.09; accepted 05.1.10; Edited by V De Laurenzi; published online 05.2.10

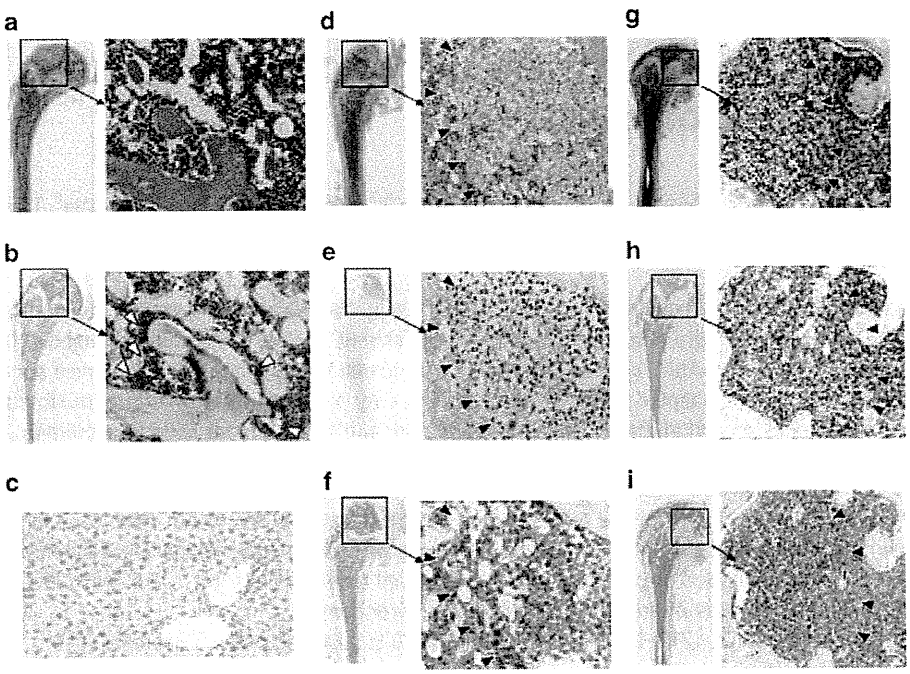

Figure 1 Engraftment of human Bcr-Abl$^+$ leukemic cells in mice. The femur of a non-engrafted mouse was stained with (**a**) hematoxylin–eosin (H&E) and (**b**) anti-pimonidazole (Ab), and the (**c**) liver was stained with anti-pimonidazole. In (**a**), the bone marrow (BM) was populated by normal mouse hematopoietic cells, and in (**b**), only a small population of normal cells was positive for pimonidazole (open triangles, Δ) along the endosteum. In (**c**), no hepatic cells were positive for pimonidazole. The femur of a K562-engrafted mouse was stained with (**d**) H&E, (**e**) antihuman Ki-67 or (**f**) anti-pimonidazole. In (**d**), the epiphysis of the bone was populated by engrafted chronic myeloid leukemia (CML) cells (closed triangles, ▲). In (**e**), the area of Ki-67-positive cells (closed triangles) was in good agreement with the area of engrafted CML cells in (**d**). Most of the engrafted CML cells were positive for Ki-67, but a few cells were negative. In (**f**), most of the engrafted CML cells (encircled by closed triangles, ▲) were positive for pimonidazole. The femur of a mouse engrafted with primary Bcr-Abl$^+$ leukemic cells from a Ph$^+$ acute lymphoblastic leukemia (Ph$^+$ ALL) patient was stained with (**g**) H&E, (**h**) antihuman Ki-67 or (**i**) anti-pimonidazole

Results

Bcr-Abl$^+$ cells in the BM survive in hypoxic conditions. Four NOD/SCID/γ_c^{null} (NOG) mice were inoculated with 1.0×10^6 K562 cells, a human cell line established from a Bcr-Abl$^+$ CML patient. Mice were killed 35 days after transplantation and examined for engraftment. Viable K562 engraftments in the BM were identified in three of the four mice. In the mouse with failed engraftment (Figure 1a), only a small population of normal cells were positive for pimonidazole, which specifically accumulates in hypoxic cells (<1.3% O_2 concentration) along the endosteum (Figure 1b). Liver cells from this were also negative for pimonidazole (Figure 1c). The transplanted K562 cells initially populated the epiphysis in recipient NOG mice. The engrafted cells were easily distinguished from normal mouse hematopoietic cells by their larger size and prominent nuclei (Figure 1d). Immunohistochemical staining with an antibody specific for human Ki-67, which is expressed in actively cycling but not quiescent cells (G_0) (Figure 1e),[22] also confirmed that K562 cells were successfully engrafted. The area of Ki-67-positive staining was in good agreement with the engraftment area estimated by cell morphology (Figures 1d and e). Although most of the engrafted cells were positive for Ki-67, a few cells were not (Supplementary Figure 2), suggesting that some engrafted K562 cells may have entered a quiescent G_0 state.[22] The majority of engrafted K562 cells were also positively labeled by pimonidazole (Figure 1f). Next, we engrafted NOD/SCID mice with primary Bcr-Abl$^+$ cells from a Ph$^+$ acute lymphoblastic leukemia (Ph$^+$ ALL) patient. Engrafted primary Bcr-Abl$^+$ cells (Figure 1g) were very similar to engrafted K562 cells (Figures 1e and f) in Ki-67 expression and pimonidazole staining (Figures 1h and i). These results indicate that both the engrafted Bcr-Abl$^+$ cell line K562 and the primary leukemic cells survive in the severely hypoxic conditions of the BM.

HA-CML cell lines. To generate hypoxia-adapted (HA)-CML cells, four CML-derived cell lines, K562, KCL22, BV173 and MYL, were continuously cultured under hypoxic conditions (1.0% O_2). Most cells were arrested in the G_1 phase of the cell cycle 2 days after transfer to hypoxic conditions as shown by an increase in the percentage of sub-G_1 cells in all four cell lines. Most of these cells underwent apoptosis within 7 days, and none of the BV173 or MYL cells survived more than 7 days (Supplementary Figure 3). In contrast, a small fraction of K562 and KCL22 cells survived in 1.0% O_2 for more than 7 days. We isolated these HA sublines of K562 and KCL22 (termed K562/HA and KCL22/HA, respectively), and these cells continued to proliferate under 1.0% O_2 for more than a year (Figures 2a and b). The

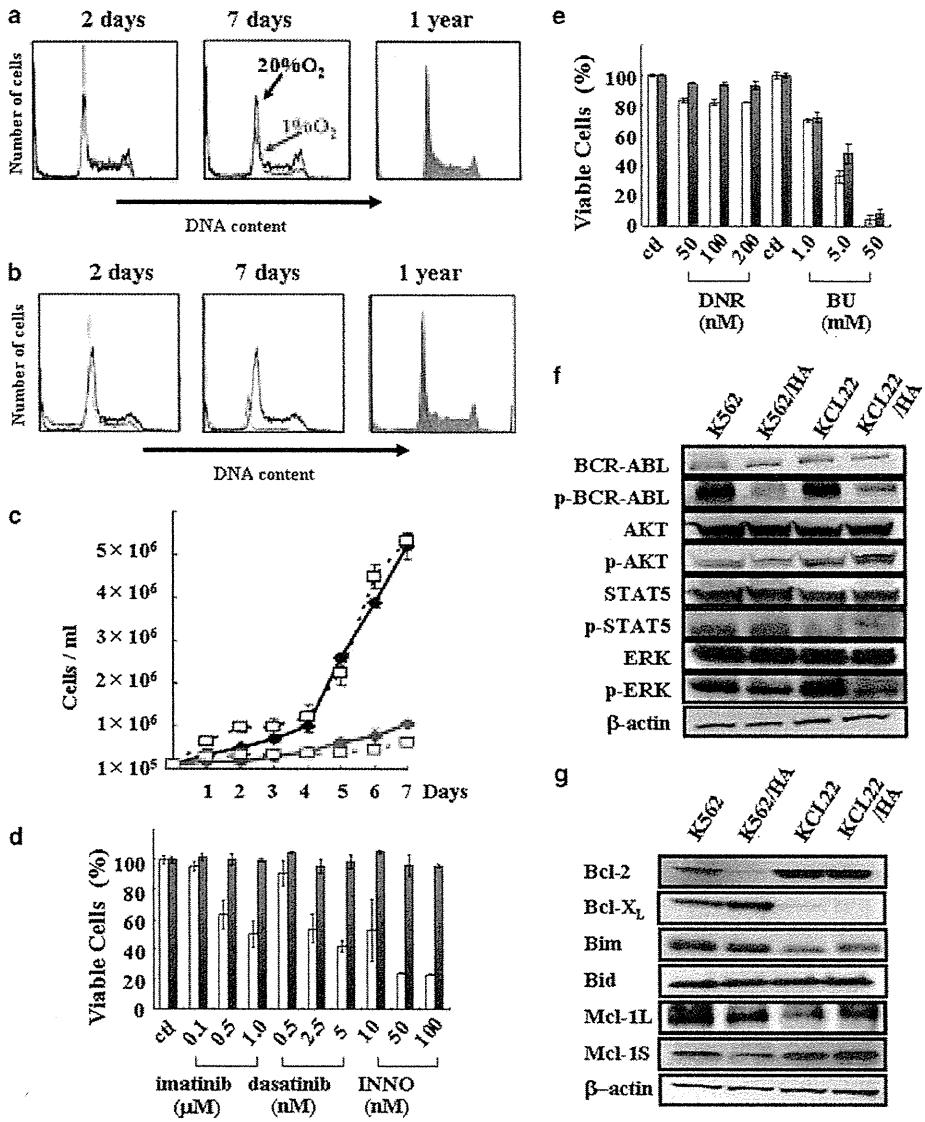

Figure 2 Characteristics of hypoxia-adapted chronic myeloid leukemia (HA-CML) cells. DNA histograms of (**a**) K562 and (**b**) KCL22 cells incubated in 1.0% O_2 (red) and 20% O_2 (blue) for 2 days, 7 days and 1 year. (**c**) Growth of K562 (blue, solid line), K562/HA (red, solid line), KCL22 (blue, broken line) and KCL22/HA (red, broken line) cells. K562 and KCL22 cells were cultured in 20% O_2, and K562/HA and KCL22/HA cells were cultured in 1.0% O_2. Antiproliferative effects of the indicated concentrations of (**d**) Abl tyrosine kinase inhibitors (TKIs) and (**e**) alkylating agents on parental K562 (white column) and K562/HA (black column) cells. (**f**) Protein expression and phosphorylation of Bcr-Abl and related kinases in parental CML cell lines and the corresponding HA subclones. (**g**) Protein levels of the indicated anti- and proapoptotic molecules in parental CML cell lines and the respective HA subclones

growth rate of both HA-CML cell lines *in vitro* was slower than that of the corresponding parental cells. Although the cell cycle distribution of both the HA cell lines was similar to that of the parental cell lines after 1 year (Figures 2a and b), the growth of the HA-CML cells was still much slower than their respective parental cell lines (Figure 2c).

We next examined the cytotoxic effects of the Abl TKIs, including imatinib, dasatinib and INNO-406, on K562, K562/HA, KCL22 and KCL22/HA cells. K562/HA cells were highly resistant to all Abl TKIs examined, compared with the parental K562 cells (Figure 2d, Table 1). As the parental KCL22 cells are intrinsically resistant to imatinib and INNO-406, we examined the antiproliferative effects of dasatinib, which has higher affinity for Abl than the other Abl TKIs, in KCL22 and KCL22/HA cells. KCL22/HA cells were approximately 50-fold less sensitive to dasatinib than the parental KCL22 cells (Table 1). Both K562/HA and KCL22/HA cells were less sensitive to the alkylating agents daunorubicin and busulfan than the respective parent cells (Figure 2e, Table 1). These results indicate that the K562/HA and KCL22/HA cells acquired resistance to a wide range of antileukemia agents during adaptation to hypoxia.

Table 1 IC_{50} scores of tyrosine kinase inhibitors, alkylating agents and Glo-I inhibitors for human CML cell lines and their hypoxia-adapted (HA) subclones

	K562	K562/HA	KCL22	KCL22/HA
ABL TKIs				
Imatinib (nM)	900	7400	—	—
Dasatinib (nM)	3.6	8.9	46.2	2264
INNO-406 (nM)	10.7	142.6	—	—
Alkylating agents				
Daunorubicin (nM)	—	—	105	954.3
Busulfan (mM)	2.4	4.5	2.2	3.0
Glo-I inhibitor				
BBGC (μM)	21.6	5.7	40.7	12.6
COTC (μM)	45.9	16.8	29.6	17.9
m-GFN (μM)	>300	230.2	>300	174.2

BBGC, *S-p*-bromobenzyl glutathione cyclopentyl diester; CML, chronic myeloid leukemia; COTC, 2-crotonyloxymethyl-4,5,6-trihydroxycylohex-2-enone; Glo-I, glyoxalase-I; TKI, tyrosine kinase inhibitor

The levels of phosphorylation of Bcr-Abl and its downstream effector Erk were reduced in K562/HA and KCL22/HA cells under hypoxic conditions (1.0% O_2), compared with levels in the parental cells cultured in normoxic conditions. The levels of phosphorylated Akt (p-Akt) and Stat5 (p-Stat5) were similar in both HA and parental cells (Figure 2f). We examined the levels of apoptosis-related proteins such as Bcl-2, Bcl-xL, Bim, Bad, Mcl-1L and Mcl-1S. The levels of Bcl-2 were lower in K562/HA cells than in K562 cells, whereas the levels of Bcl-xL were higher. Bim and Bid interact with Bcl-2 and Bcl-xL to induce apoptosis. The levels of Bim and Bid in K562/HA cells were not different from those in the parental cells. The level of the antiapoptotic Mcl-1L was the same in K562/HA and parental cells, whereas the level of the proapoptotic Mcl-1S decreased in K562/HA cells (Figure 2g). In contrast to K562 and K562/HA cells, there were no differences between KCL22 and KCL22/HA cells (Figure 2g). These findings suggest that adaptation to hypoxia may have some impact on the mechanisms for executing apoptosis, although further investigation will be required to confirm this hypothesis.

Glo-I in HA-CML cells. We examined the ATP levels in parental and HA-CML cells. The amounts of ATP in K562/HA and KCL22/HA cells were 73.0 and 93.2%, respectively, of the levels in their respective parental cell lines under normoxia (Figure 3a). In addition, both HA cell lines exhibited high levels of glucose consumption and lactate production compared with their respective parental cells (Supplementary Figure 4). Normally, one molecule of glucose produces approximately 34–36 ATPs by aerobic respiration, but only 2 ATPs by glycolysis (Figure 3b). Our results suggest that anaerobic glycolysis generates sufficient ATP for survival of HA-CML cells in hypoxic conditions.

When cells preferentially use glycolysis for energy production, glycolysis-specific cytotoxic by-products, such as methylglyoxal, accumulate intracellularly. As glyoxalase-I (Glo-I) protects cells and promotes cell survival by detoxifying methylglyoxal (Figure 3b), we examined Glo-I in HA-CML cells. Both K562/HA and KCL22/HA cells had higher Glo-I protein levels (Figure 3c) and enzymatic activity (Figure 3d) than the parental cells. Furthermore, the Glo-I protein level increased markedly in the parental K562 cells after cultivation in 1.0% O_2 for 28 days (Figure 3e). In addition, we examined the Glo-I protein levels in primary Bcr-Abl$^+$ cells from CML and Ph$^+$ ALL patients. Both samples of primary Bcr-Abl$^+$ cells possessed higher Glo-I protein levels than normal BM or PB cells (Supplementary Figure 5). These findings indicate that Glo-I expression was induced not only in the artificially generated HA-CML cell lines but also in primary Bcr-Abl$^+$ cells, suggesting that primary leukemic cells may be adapted to hypoxia *in vivo*.

High Glo-I expression is sustained in HA-CML cells after 6 months in normoxia. The HA cells returned to normoxic culture conditions revert to the parental cell proliferation rate after 5 days (Supplementary Figure 6a), and the fraction of cells in G_0 decreases within 48 h after return to normoxic conditions (Supplementary Figure 6b). Interestingly, the high level of Glo-1 expression developed by HA-CML cells was sustained after 6 months in culture under normoxic conditions (Supplementary Figure 6c).

Engraftment of HA-CML cells in NOG mice. We established stable subclones of K562 and K562/HA cells ($K562^{Luc\text{-}EGFP}$ and $K562/HA^{Luc\text{-}EGFP}$, respectively) that coexpressed luciferase and enhanced green fluorescent protein (EGFP). When we examined the bioluminescence of the cells, $K562^{Luc\text{-}EGFP}$ cells produced approximately 10 times more bioluminescence than did $K562/HA^{Luc\text{-}EGFP}$ cells (Figure 4a). As the strength of luciferase bioluminescence depends on the availability of ATP and oxygen, we hypothesized that these factors may have a role in the reduced bioluminescence of $K562/HA^{Luc\text{-}EGFP}$ cells. Engraftment and proliferation of $K562^{Luc\text{-}EGFP}$ and $K562/HA^{Luc\text{-}EGFP}$ cells in NOG mice were monitored using *in vivo* imaging (Figure 4a). Despite the lower level of bioluminescence in $K562/HA^{Luc\text{-}EGFP}$ cells in culture, there were no significant differences in total photon emission between $K562^{Luc\text{-}EGFP}$- and $K562/HA^{Luc\text{-}EGFP}$-engrafted mice before day 34. After day 34, the total photon emission of $K562/HA^{Luc\text{-}EGFP}$-engrafted mice increased much more sharply than that of $K562^{Luc\text{-}EGFP}$ mice (Figure 4b). In addition, $K562/HA^{Luc\text{-}EGFP}$-transplanted mice died significantly earlier than did $K562^{Luc\text{-}EGFP}$ mice (Figure 4c). These results indicate that $K562/HA^{Luc\text{-}EGFP}$ cells engrafted more efficiently in NOG mice than did the parental $K562^{Luc\text{-}EGFP}$ cells.

To investigate why $K562/HA^{Luc\text{-}EGFP}$ cells engrafted more efficiently, we examined the cell cycle distribution of K562 and K562/HA cells. The percentages of cells in G_0 in K562 and K562/HA cells were $0.87 + 0.58$ and $4.9 + 2.1$%, respectively, indicating that the K562/HA grafts included more quiescent cells than did the parental line (Figures 4d and e). Next, we examined the expression of c-kit, Tie-2, CXCR4, Notch, N-cadherin, VLA-4, LFA-1 and CD44, all of which have been reported to indicate stemness.[23] There was no difference in the expression levels of these proteins in K562/HA or KCL22/HA cells and the respective parental cell lines (data not shown). Interestingly, both HA cell lines expressed higher levels of β-catenin, which is thought to be important for

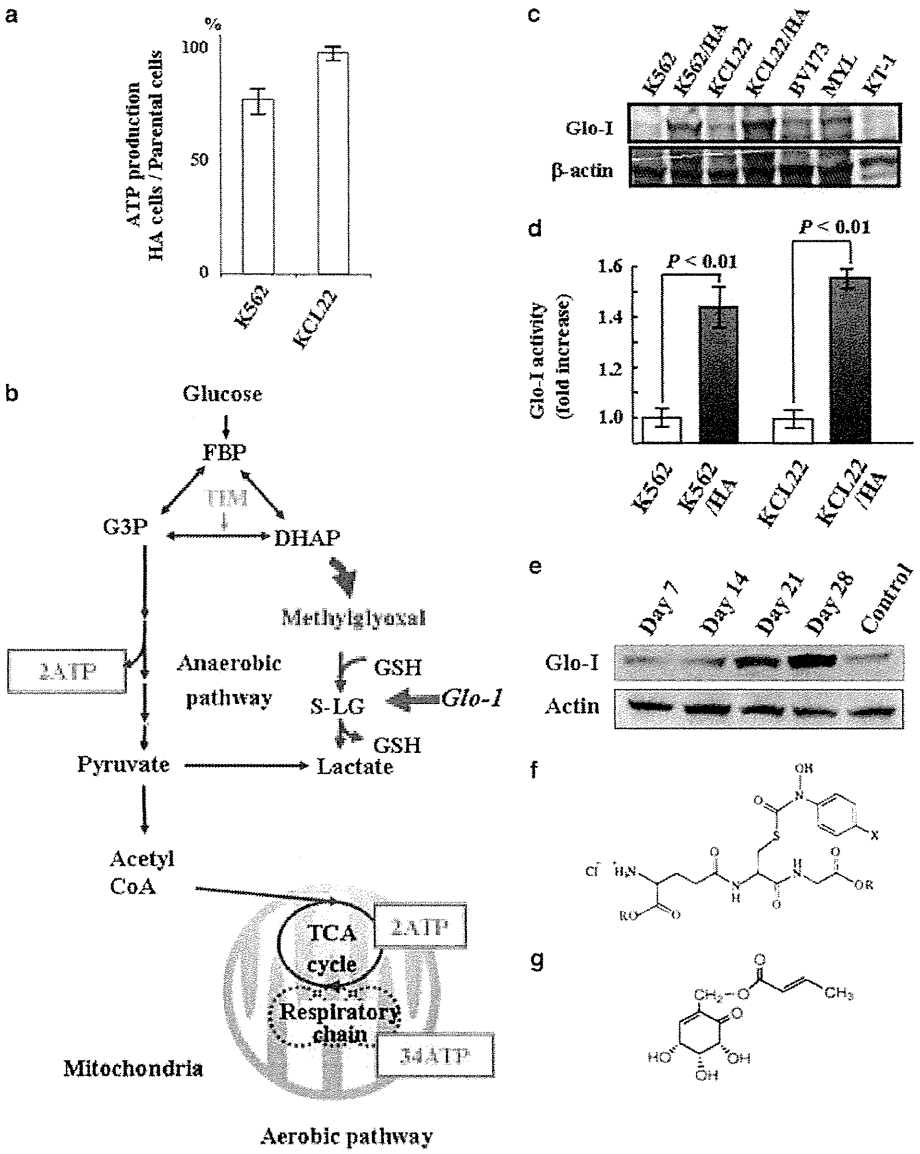

Figure 3 The influences of adaptation to hypoxia on ATP production and glyoxalase-I (Glo-I) activity. (**a**) ATP production is expressed as the ratio of production in hypoxia-adapted (HA) cells relative to parental chronic myeloid leukemia (CML) cells. (**b**) Schematic illustration of aerobic and anaerobic ATP production pathways. Methylglyoxal accumulates in cells that use the anaerobic pathway, and Glo-I functions to detoxify methylglyoxal. (**c**) Glo-I protein levels in parental CML cell lines and the respective HA subclones. (**d**) Glo-I activity in parental CML cell lines and the respective HA subclones. (**e**) Glo-I protein levels under hypoxic conditions. Glo-I expression was clearly evident 21 days after initiation of hypoxia (1.0% O_2). Chemical structures of *S-p*-bromobenzyl glutathione cyclopentyl diester (BBGC) (**f**) and 2-crotonyloxymethyl-4,5,6-trihydroxycylohex-2-enone (COTC) (**g**)

production of CML stem cells (Figure 4f).[24] In addition, the K562/HA cell line contained more cells with the side population marker for cancer stem cells (Figure 4g).[25] These findings suggest that the adaptation to hypoxia induces putative stem/progenitor cell-like characteristics in Bcr-Abl$^+$ cells.

Effect of Glo-I inhibitors on HA-CML cells. *S-p*-bromobenzyl glutathione cyclopentyl diester (BBGC) (Figure 3f) is a specific cell-permeable inhibitor of Glo-I,[26] and 2-crotonyloxymethyl-4,5,6-trihydroxycylohex-2-enone (COTC) (Figure 3g) is an inhibitor of Glo-I and glutathione.[27] Recently, methyl-gerfelin (Supplementary Figure 7a) was also identified as a Glo-I inhibitor.[28] Although HA-CML cells were resistant to the cytotoxic effects of Abl TKIs and alkylating agents (Figures 2d and e, Table 1), BBGC, COTC and methyl-gerfelin were more strongly cytotoxic in K562/HA and KCL22/HA cells than in the parental cell lines (Figures 5a–d, Supplementary Figures 7b and c).

To determine the mechanism of cell death induced by BBGC, we examined Annexin V staining (Supplementary

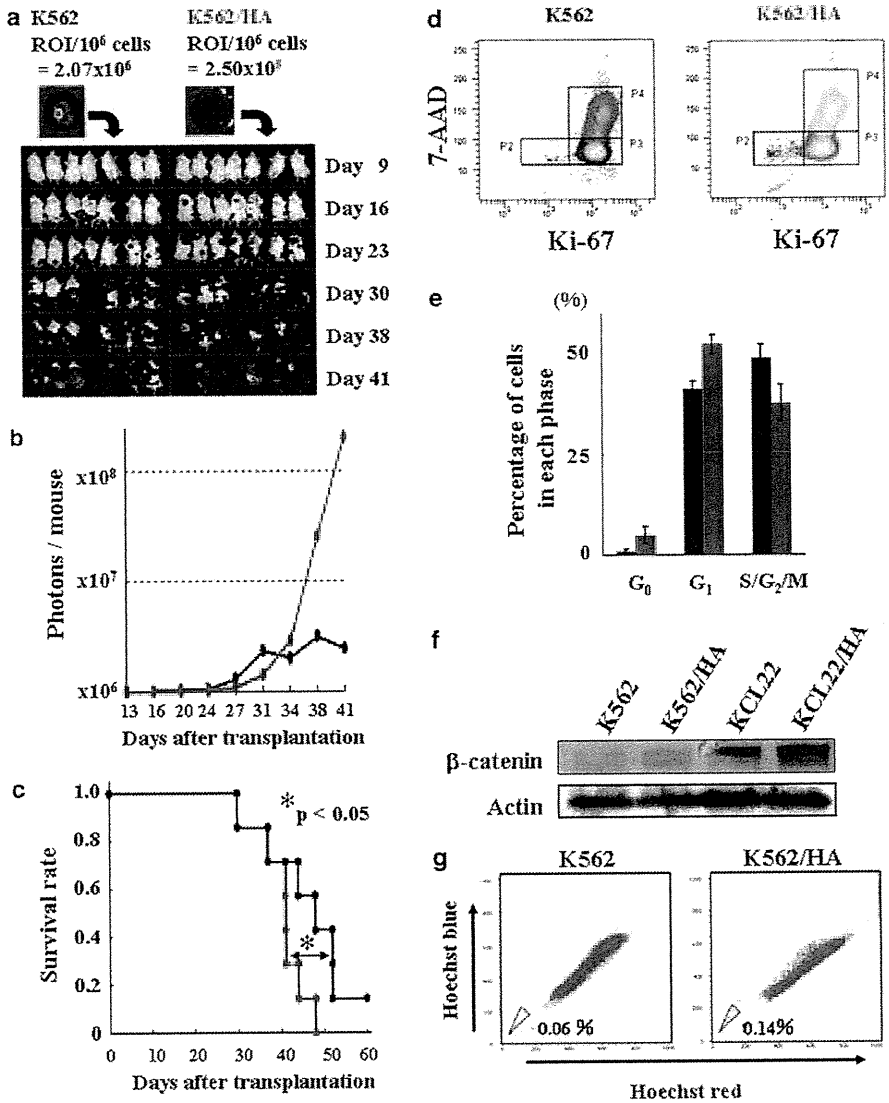

Figure 4 K562/hypoxia-adapted (HA) cells engraft more efficiently in NOD/SCID/γ_c^{null} (NOG) mice. (**a**) Whole animal experiments using NOG mice inoculated with K562$^{Luc\text{-}EGFP}$ or K562/HA$^{Luc\text{-}EGFP}$ cells. Engraftment was monitored by *in vivo* imaging. (**b**) Total photon emission from mice inoculated with K562$^{Luc\text{-}EGFP}$ (blue) or K562/HA$^{Luc\text{-}EGFP}$ (red) cells. (**c**) Survival rates of mice inoculated with K562$^{Luc\text{-}EGFP}$ (blue) or K562/HA$^{Luc\text{-}EGFP}$ (red) cells. (**d**) Cell cycle distributions of K562 and K562/HA determined by double staining with Ki-67 and 7-AAD. (**e**) The percentages of cells in each phase of the cell cycle in K562 (blue) and K562/HA (red), (**f**) β-catenin protein expression levels in K562, K562/HA, KCL22 and KCL22/HA cells. (**g**) Number of side population cells in K562 and K562/HA cells

Figures 8a–d) and mitochondrial outer membrane permeabilization (Supplementary Figures 8e–h). The proportion of cells undergoing apoptosis was greater in the BBGC- and COTC-treated K562/HA and KCL22/HA cells than in the parental cells (Supplementary Figures 9a–d). These results indicate that HA-CML cells were dependent on Glo-I activity for survival under hypoxic conditions, whereas the parental cells, cultured in normoxic conditions, were not dependent on Glo-I activity.

To evaluate the *in vivo* antileukemic activity of BBGC, we treated NOG mice inoculated with K562$^{Luc\text{-}EGFP}$ or K562/HA$^{Luc\text{-}EGFP}$ cells with BBGC. BBGC had no apparent effect on the survival of K562$^{Luc\text{-}EGFP}$-engrafted mice (Figure 5e). However, it significantly prolonged the survival of K562/HA$^{Luc\text{-}EGFP}$-transplanted mice (Figure 5f). The body weight of BBGC-treated mice did not decrease during the course of treatment (data not shown). These findings indicate that BBGC has potent antileukemic effects *in vivo*, and preferentially targets CML cells with higher Glo-I activity, with minimal associated toxicity.

Discussion

Abl TKIs can induce apoptosis only in actively proliferating Bcr-Abl$^+$ cells, making these drugs much less active against CML stem cells, which are predominantly in a quiescent